buildings

MDPI

Article

The Impact of Ground-Floor Elevation of School Buildings on Courtyard Wind Environment

Qiang Wen *, Haiqiang Liu, Qiang Zhou, Qinghai Guo, Pinliang Wang and Luyao Zhang

School of Civil Engineering and Architecture, Zhejiang Sci-Tech University, Hangzhou 310018, China; liu.haiqiang@zstu.edu.cn (H.L.); zhouqiang@zstu.edu.cn (Q.Z.); qhguo@zstu.edu.cn (Q.G.)
* Correspondence: architectwq@zstu.edu.cn

Abstract: Poor wind conditions in metropolitan areas can result in inadequate ventilation and degradation of the thermal environment. Several researches have demonstrated that the building ground floor elevation (BGFE) enhances the wind conditions surrounding buildings. Further investigation is required to thoroughly examine the BGFE's impact on the wind conditions in the courtyard area. We researched how the various overhead placements affect the ventilation of a U-shaped school building's courtyard space in different wind directions. We performed Computational Fluid Dynamics (CFD) numerical simulation experiments on 93 overhead scenarios based on field measurements and validation. The statistical analysis of the experimental data revealed that the BGFE had significant effects on reducing the mean air age ($p < 0.001$), standard deviation of air age ($p < 0.01$), standard deviation of wind speed ($p < 0.001$), and mean wind speed ($p < 0.01$) in the courtyard space. The BGFE in the northeastern zone of the U-shaped school building significantly increased the mean air age ($p < 0.05$), while the BGFE in the middle and southwestern zones significantly decreased the mean air age ($p < 0.001$), and the BGFE in the southeastern zone significantly decreased the mean wind speed ($p < 0.05$). The BGFE facilitates the entry of fresh air and offers even ventilation while significantly reducing wind speed. Choose sites C and D to enhance the U-shaped courtyard's ventilation and avoid locations B and E. This paper's findings provide theoretical guidance for designing the elevation of courtyard space from a ventilation perspective and for the green rehabilitation of existing buildings.

Keywords: elevation; wind environment; ventilation; courtyard; school building

Citation: Wen, Q.; Liu, H.; Zhou, Q.; Guo, Q.; Wang, P.; Zhang, L. The Impact of Ground-Floor Elevation of School Buildings on Courtyard Wind Environment. *Buildings* **2024**, *14*, 1146. https://doi.org/10.3390/buildings14041146

Academic Editor: Theodore Stathopoulos

Received: 15 March 2024
Revised: 16 April 2024
Accepted: 16 April 2024
Published: 18 April 2024

1. Introduction

The concept of creating appropriate microclimates in urban areas is gaining attention in the context of urban warming and the heat island effect. Developing suitable community microclimates can promote outdoor activities, benefiting individuals' physical and mental well-being [1]. Urban wind conditions impact urban ventilation, air quality, and pedestrian comfort and safety [2–5]. Elevated ground floors [6–10] and openings [11–13] are often used in architectural design to improve urban ventilation and create a suitable living environment. The building ground floor elevation (BGFE) typically raises a portion of, or the entire ground floor of a structure, creating a semi-open space for social activities while maintaining structural columns and vertical transportation areas [14]. Several studies have demonstrated that BGFE can improve wind speed and comfort at the pedestrian level [7–10,15], promoting ventilation and pollutant dispersion [16].

The BGFE of single isolated buildings can have varying impacts on the pedestrian wind environment in and around the elevation area due to factors such as elevation [7], building aspect ratio [17,18], center core width [19], wind direction [6,19], and the size of the study area [20]. The BGFE can improve wind comfort around conventionally [6] and unconventionally designed structures [20]. Elevations in short and wide structures can create a greater pedestrian wind comfort zone, but tall, thin, raised buildings have just a

small area of suitable wind conditions [17,18]. The width of the elevation core controls the low wind speed zone [19], while the elevation's height determines the size of the high and low wind speed zones around the building [7]. The elevation can create different wind environment impacts in multiple building assemblies due to building spacing [21], porosity [12], and building form relationships [22]. The elevation design can improve the low wind speed zone at the pedestrian level of row buildings, but it may not necessarily improve the wind environment at the pedestrian level of row buildings with podiums [8]. It can also significantly improve the pedestrian wind environment around the building for a specific building spacing [21]. The building matrix's larger porosity formed by elevation has better wind comfort than smaller porosity [12]. Increasing building height, removing upstream buildings, and making the target building taller or shorter than the upstream building can improve wind comfort in the lift zone [22].

The BGFE has a positive effect on ventilation, thermal comfort, and pollution dispersion in street canyons [9,23,24], which can be influenced by the height of the elevation [25], the height and the spacing of the buildings [18], and other morphological factors. Void decks in 2D symmetric street canyons have a significant effect on airflow structure and pollutant dispersion within the street canyon [23]; variations in the width–height ratio of a 2D street canyon have a smaller effect on wind enhancement than variations in the height of an empty deck [25]. Void decks in three-dimensional urban street canyons can greatly increase pedestrian-level wind speeds compared to non-void decks [9]. They can significantly improve ventilation performance in asymmetrical canyons [26] and reduce pollutant levels in long canyons [24]. In ideal urban canyons with elevation, average wind speed is negatively related to building height [18]. Elevation design in residential buildings can greatly enhance the pedestrian wind conditions in residential regions [27]. Various building design variables such as elevation form, height, and location of the elevated envelope can affect pedestrian thermal comfort in a high-rise residence's ground floor elevation area [28]. The elevation at both ends and in the middle of the dwelling significantly increases the mean velocity ratio (MVR) in the elevated area [29].

There are few studies on the impact of overhead design on the campus environment. Using a lift-up design on campuses can effectively improve the pedestrian horizontal wind environment and thermal comfort, providing a comfortable summer microclimate without creating strong winter stress [15]. Building openings and elevation designs can increase the acceptable wind comfort area on university campuses from 20% to 50% [13]. Today, courtyard spaces are heavily used in campus buildings. A courtyard is an enclosed or semi-enclosed area that is surrounded by buildings and open to the sky. Architects typically incorporate courtyards into their designs to facilitate natural ventilation and temperature control by ensuring they are connected to the environment to get sunlight and fresh air [30]. The wind conditions play a crucial role in the microclimate of courtyards, impacting pollutant dispersion, thermal comfort, and the energy efficiency of buildings. Courtyard form is related to the wind environment [31], and its aspect ratio affects the airflow pattern in the courtyard [32]. The ideal aspect ratios for air quality and ventilation in parallel courtyards lie within the range of 1–2 [33]. Semi-enclosed courtyards positively impact the thermal environment based on their orientation [34]. Installing openings can enhance air exchange efficiency in courtyards [35]. Placing openings on the leeward side of a building increases the cross-ventilation rate with building height [36]. Few of these related studies have investigated the effect of elevated design on the spatial microclimate of courtyards from the microscale of school building courtyards.

The U-shaped courtyard has become a frequently used spatial pattern for school buildings due to its convenient transportation, good lighting and ventilation, and the creation of a semi-enclosed space. The school building courtyard is the main after-school activity space for students. Creating a favorable wind environment promotes student engagement in outdoor activities, benefiting their physical and mental well-being, improving their satisfaction with the school building courtyard, and lowering the likelihood of learning anxiety [37]. The BGFE of a courtyard building enhances spatial hierarchy, offers a panoramic

perspective of the landscape, and creates a sheltered outdoor space for various activities. The elevation design typically focuses on specific localized areas rather than the entire first floor. Further investigation is required to understand how ground floor elevation affects the wind conditions in courtyard spaces and the varying effects of different elevation positions.

In summary, previous research has primarily focused on analyzing the impact of the BGFE on the wind environment in various settings, such as individual buildings [6,7], rows of buildings [10,15,16], urban street canyons [9,26], and residential areas [27–29]. Most have been in the wind environment in elevated areas [19,28] or around buildings [27,29]. Few researchers have examined the microclimate of courtyard spaces [33], and there is limited research on the wind conditions in U-shaped courtyards [6]. Research primarily focuses on how factors such as building height [12,17,18], overhead height [7,18,22,28], and the size and shape of the center core [17,19] influence the wind environment in elevated areas and their surroundings. Some scholars have studied the effects of elevation location [29] on the wind environment of the pedestrian level around the residential community. Further research is needed on the location factors of the courtyard building overhead. There needs to be more research that examines the impact of overhead design on the wind environment of courtyard spaces from the micro perspective of academic buildings. In addition, most evaluation systems concerning the wind environment focus on parameters such as wind speed [29], wind speed ratio [6,7,29], and air age [33], and there needs to be a more comprehensive evaluation of these indicators and their discrete degrees.

This research uses the climatic conditions of locations with hot summers and cold winters as a case study. It takes the No. 2 teaching building of Zhejiang Sci-Tech University as the research prototype of a "U"-shaped architectural courtyard (Figure 1) to study the influence mechanism of different overhead design locations on the courtyard space's wind environment under different wind directions. The main research objectives of this paper are as follows: 1. What is the overall effect of the BGFE on the wind environment indicators of the "U"-shaped courtyard? 2. How does elevation in different locations affect the wind environment indicators of the "U"-shaped courtyard? 3. What is the correlation between the wind environment indicators of the "U"-shaped courtyard formed by elevation?

(**a**) (**b**)

Figure 1. Aerial photos of Zhejiang Sci-Tech University. (**a**) Overall aerial view of Zhejiang Sci-Tech University. (**b**) Aerial photo of No. 2 teaching building of Zhejiang Sci-Tech University.

The rest of the paper is divided as follows: Section 2 describes the methodology used in this study, including a description of the experimental cases and evaluation criteria, the CFD simulation methodology, and the simulation validation study. Section 3 presents the data and statistical analysis of the experimental results. Section 4 is an analysis and discussion of the experimental statistical results, and describes the limitations of the article. Section 5 is the concluding remarks, which summarize this study's main findings and implications, and directions for further work.

2. Methodology

2.1. Courtyard Elevation Pattern

This work uses the No. 2 teaching building of Zhejiang University of Science and Technology (Figure 1) as a prototype. We identified five distinct elevated positions (labeled a, b, c, d, e) on the U-shaped building and analyzed the various combinations of these positions under three wind directions: southwest, southeast, and south (Figure 2). There were 31 combinations for each wind direction (Table 1), resulting in a total of 93 cases. The simulation of these samples was proposed to investigate the overall effect of different elevation locations on the pedestrian-level wind environment indicators of the courtyard space under different wind directions, as well as the correlation between the wind environment indicators of the courtyard. To succinctly describe and analyze the experiment's results, the courtyard space at pedestrian height is split into Area I, Area II, Area III, and Area IV based on their positions (Figure 2). The term "courtyard" refers to the "U-shaped courtyard" in the descriptions.

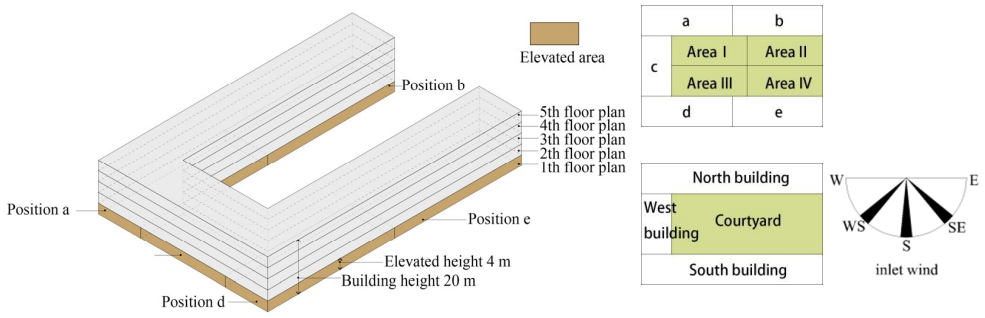

Figure 2. U-shaped courtyard experimental subjects. (**a**) U-shaped courtyard axonometric drawing. (**b**) Courtyard zoning. (**c**) Study winds.

Table 1. Examples of elevated locations in "U"-shaped courtyards.

One position elevated	A	B	C	D	E
Two positions elevated	Ab	Ac	Ad	Ae	Bc
	Bd	Be	Cd	Ce	De
Three positions elevated	Abc	Abd	Abe	Acd	Ace
	Ade	Bcd	Bce	Bde	Cde
Four positions elevated	Abcd	Abce	Abde	Acde	Bcde
All elevated	Abcde				

2.2. Research Indicators

Wind speed, wind speed standard deviation, air age, and air age standard deviation were used as performance indicators to analyze wind fields. The paper standardized the wind environment data of the elevated design to study the impact of the BGFE on the courtyard space. That involved comparing the rate of change of wind environment indexes between the elevated and un-elevated cases, as presented in Table 2. In addition, this study was conducted to investigate the wind environment at the pedestrian height of the courtyard space, so all the wind environment indicators refer to the 1.5 m height of the courtyard space.

Table 2. Glossary.

V	Air velocity	Ag	Air age
MV	Mean wind velocity of the courtyard	MA	Mean air age of the courtyard
ΔMV	Rate of change of mean wind velocity	ΔMA	Rate of change of mean air age
MV_{mean}	Mean value of average wind speeds	MA_{mean}	Mean value of average air age
ΔMV_{mean}	Mean value of the rate of change of the average wind speed	ΔMA_{mean}	Mean value of the rate of change in mean air age
Vσ	Standard deviation of wind speeds of the courtyard	Aσ	Standard deviation of air age of the courtyard
ΔVσ	Rate of change of standard deviation of wind speeds	ΔAσ	Rate of change of standard deviation of air age
$V\sigma_{mean}$	Mean value of standard deviation of wind speeds	$A\sigma_{mean}$	Mean value of standard deviation of air age
$\Delta V\sigma_{mean}$	Mean value of the rate of change of the standard deviation of wind speeds	$\Delta A\sigma_{mean}$	Mean value of the rate of change of the standard deviation of the air age
SW	Southwest wind direction	$A\sigma_{med}$	Median standard deviation of air age
SE	Southeast wind direction	U	Measured wind speed
S	South wind direction	U_{ref}	Approaching wind speed
MVR	Mean wind velocity ratio	BGFE	Building ground floor elevation

Mean wind speed (MV): The average wind speed at all measurement points at the height of 1.5 m above the floor of the courtyard space.

The rate of change for the mean wind speed (ΔMV): This is the rate of change of the elevation design's mean wind speed compared to the un-elevation design's mean wind speed. The formula is:

$$\Delta MV = (MV_{LU} - MV_{NLU})/MV_{NLU} \quad (1)$$

ΔMV is the rate of change of average wind speed for a given elevation design yard, MV_{LU} is the average wind speed for a given elevation design yard, and MV_{NLU} is the average wind speed for an un-elevation yard.

Wind speed standard deviation (Vσ): In this study, the wind speed standard deviation is used to evaluate the wind speed homogeneity of pedestrian height in the courtyard space. The lower the standard deviation of wind speed, the less the dispersion of wind speed; the more uniform the distribution of wind speed, the better the wind environment.

The rate of change for the wind speed standard deviation (ΔVσ): This evaluates the tendency of wind speed uniformity to change in the courtyard space according to the elevation at different school building locations. The calculation formula is:

$$\Delta V\sigma = (V\sigma_{LU} - V\sigma_{NLU})/V\sigma_{NLU} \quad (2)$$

$V\sigma_{LU}$ denotes the standard deviation of wind speed for a particular elevated design courtyard, and $V\sigma_{NLU}$ denotes the standard deviation of wind speed for a courtyard without elevation. ΔVσ is the rate of change of the standard deviation of the wind speed in the courtyard of a specific overhead design.

Mean air age (MA): The average air age at all measurement points at a height of 1.5 m above the floor of the courtyard space. Air age is the time elapsed for air to flow into an area through an opening. It is a measure of air freshness that can also be considered an indicator of indoor air quality and ventilation efficiency [38]. A growing number of studies have applied air age to outdoor urban spaces, reflecting the ventilation efficiency of urban

spaces [3,39]. Mean air age is commonly used to assess permeability [40,41] and reflects the ventilation potential of an area. The smaller the mean air age, the fresher and better ventilated the air in the courtyard space.

The rate of change for the mean air age (ΔMA): This is the percentage change in average air age for the elevation option compared to the un-elevation option. The formula is:

$$\Delta MA = (MA_{LU} - MA_{NLU})/MA_{NLU} \quad (3)$$

where ΔMA is the rate of change in the average age of air for a given elevated design, MA_{LU} is the average age of air for a given elevated design, and MA_{NLU} is the average age of air for an un-elevation yard.

Air age standard deviation (Aσ): In this study, the air age standard deviation was used to evaluate the air age homogeneity of pedestrian height in the courtyard space. The smaller the air-age standard deviation, the lower the air-age dispersion, and the more uniform the ventilation in the courtyard.

The rate of change for the air age standard deviation (ΔAσ): This is the percentage change of air age standard deviation of the elevation scheme compared to the un-elevation scheme. It is used to evaluate the trend of change in air age uniformity of the courtyard space by different elevated location designs of the academic building. The calculation formula is:

$$\Delta A\sigma = (A\sigma_{LU} - A\sigma_{NLU})/A\sigma_{NLU} \quad (4)$$

where $A\sigma_{LU}$ denotes the standard deviation of the air age of the courtyard formed by the design of a specific elevated location, and $A\sigma_{NLU}$ denotes the standard deviation of the air age of the courtyard formed by the design of no elevated location. ΔAσ is the percentage change of the standard deviation of the age of the yard air formed by the design of a specific elevated location.

2.3. Simulation Methodology

While LES is undoubtedly more precise, it demands greater intricacy and higher costs [42]. In contrast, previous studies have extensively employed RANS approaches that prioritize the analysis of the mean flow characteristics of turbulence [43]. On the other hand, the RNG model has demonstrated enhanced efficacy in addressing intricate flow problems characterized by rotation, recirculation, and significant adverse pressure gradients [44]. The turbulence model was set as the RNG k-ε model, considering that the RNG k-ε model has better ventilation performance inside and outside the building [45]. The pressure–velocity coupling algorithm is SIMPLE, and the pressure interpolation method uses an interleaved format named PRESTO. The viscous and convective terms in the control equations are discretized using the second-order windward format. Standard wall functions are also used for building surfaces with zero roughness height. Zero gauge pressure is applied at the exit plane. Each simulation must go through more than 10,000 iterations to achieve convergence. The computational progress is terminated when the discretization error decreases and remains at a reasonable level. During this process, the residual extremes in the simulations were set to 10^{-5}. All calculations were performed by Pheonics 2019 on a 40-core workstation (Intel(R) Xeon(R) CPU E5-2673 v4, 2.3 GHz) with 96 GB DDR of system memory.

According to the relevant practice guidelines by Tominaga et al. [46], the size of the computational domain is defined by the model height "H". The computational domain's upstream, downstream, lateral, and height settings are bigger than 5H, 15H, 5H, and 5H, respectively. The dimensions of the building model are width × depth × height = 108 m × 72 m × 20 m; as shown in Figure 3a. The size of the computational domain was set to 900 m × 900 m × 120 m so that the minimum upstream distance and downstream distance of the computational domain satisfy the requirement of greater than 15H under various initial wind angles, and the height of the computational domain also satisfies the requirement of being greater than 5H. The maximum blocking rate is 2%, which is below the recommended threshold of 3% [46]. The structured cells cover the entire computational area, with the

vicinity of the building covered by a compact grid and the rest of the area filled with a sparse grid (Figure 3b).

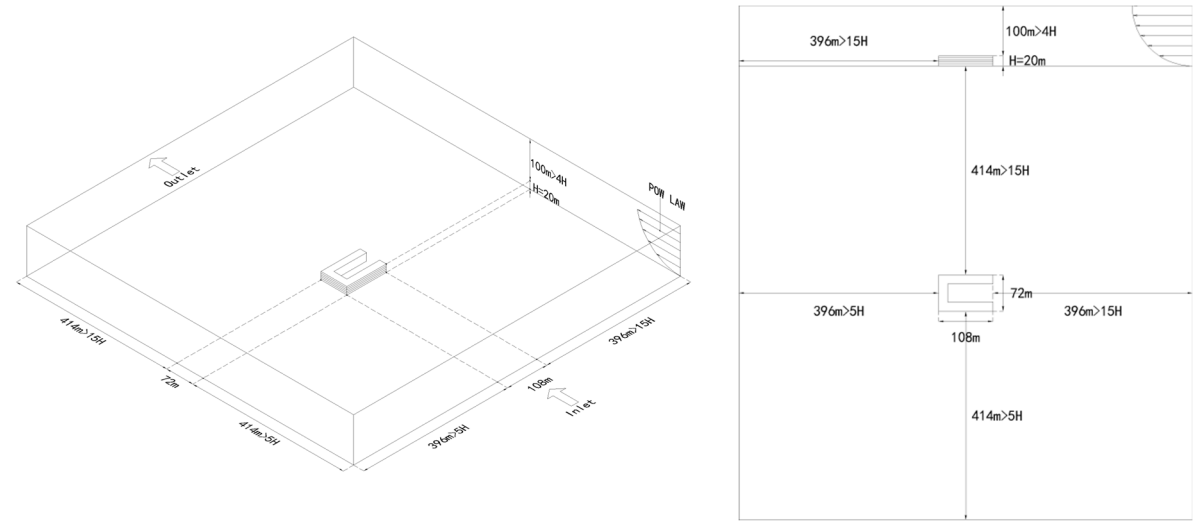

(**a**)

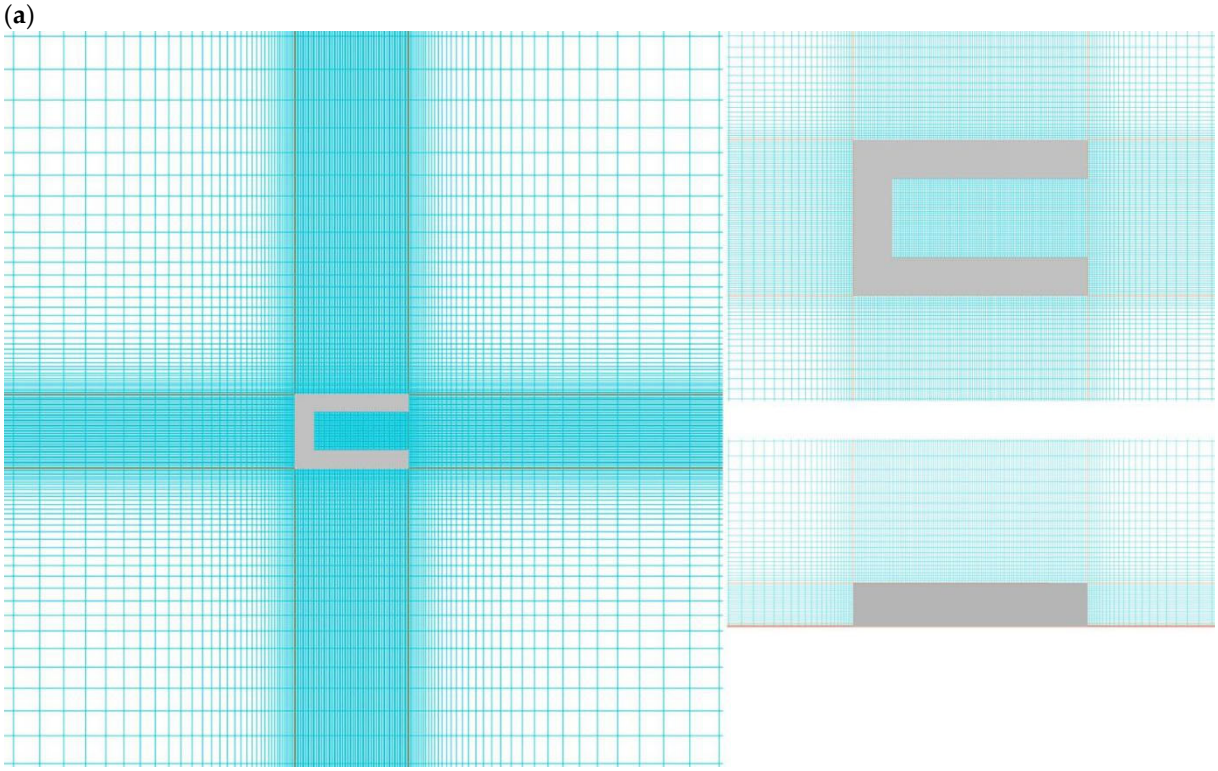

(**b**)

Figure 3. CFD simulation settings. (**a**) Calculation domain for CFD settings. (**b**) Computational domain mesh conditions.

Hangzhou, located in eastern China, is chosen as the study site, which is in the hot-summer and cold-winter climate zone. The annual average wind speed of Hangzhou is 2.4 m/s [47]. The inflow boundary profiles of the wind velocity ($U(z)$), turbulent kinetic energy ($k(z)$), and turbulent dissipation rate ($\varepsilon(z)$) can be specified by fitting Equations (5)–(7).

$$U(z)/U_{ref} = (z/H)^{\alpha} \tag{5}$$

$$k(z) = u^2/\sqrt{C_{\mu}} \tag{6}$$

$$\varepsilon(z) = C_{\mu}^{3/4} k^{3/2} / (\kappa_v z) \quad (7)$$

where H is the reference height, U_{ref} (=2.4 m/s) is the reference wind speed at that height, α is the roughness index, which is determined by the surrounding environment. Because this paper mainly studies the influence of elevation on the wind environment of the courtyard space, in order to eliminate other influencing factors, we assume that the building is located in the suburbs, corresponding to the roughness index of 0.14 [48]. C_{μ} is a constant (C_{μ} = 0.09), u^* is the friction velocity (u^* = 0.24 m/s), κ_v is von Karman's constant (κ_v = 0.41).

2.4. Grid-Independence Test

In order to balance the computational time, a grid sensitivity analysis was performed to determine the optimal grid resolution for CFD simulations. Three grid sizes with different resolutions were produced separately—fine grid (1.75 million cells), medium grid (1.37 million cells), and coarse grid (1.14 million cells)—to compare the grid sensitivity. In the west area and the south area of the school building courtyard, two test lines—L1 and L2—were placed along the horizontal and vertical directions to monitor the normalized wind speed values at three resolution grids, as shown in Figure 4a. The normalized wind speed is the ratio of the measured wind speed U to the approaching wind speed U_{ref}. As shown in Figure 4b,c, the mean absolute percentage error (MAPE) of the coarse grid from the medium grid was calculated to be 3.40%, and the MAPE of the medium grid from the fine grid was 1.61%. The medium grid is sufficient to meet the grid independence requirements, with a first grid height of 0.012 m normal to the wall and a y+ of 30 near the building wall. Therefore, the medium grid is selected as the grid resolution for further analysis.

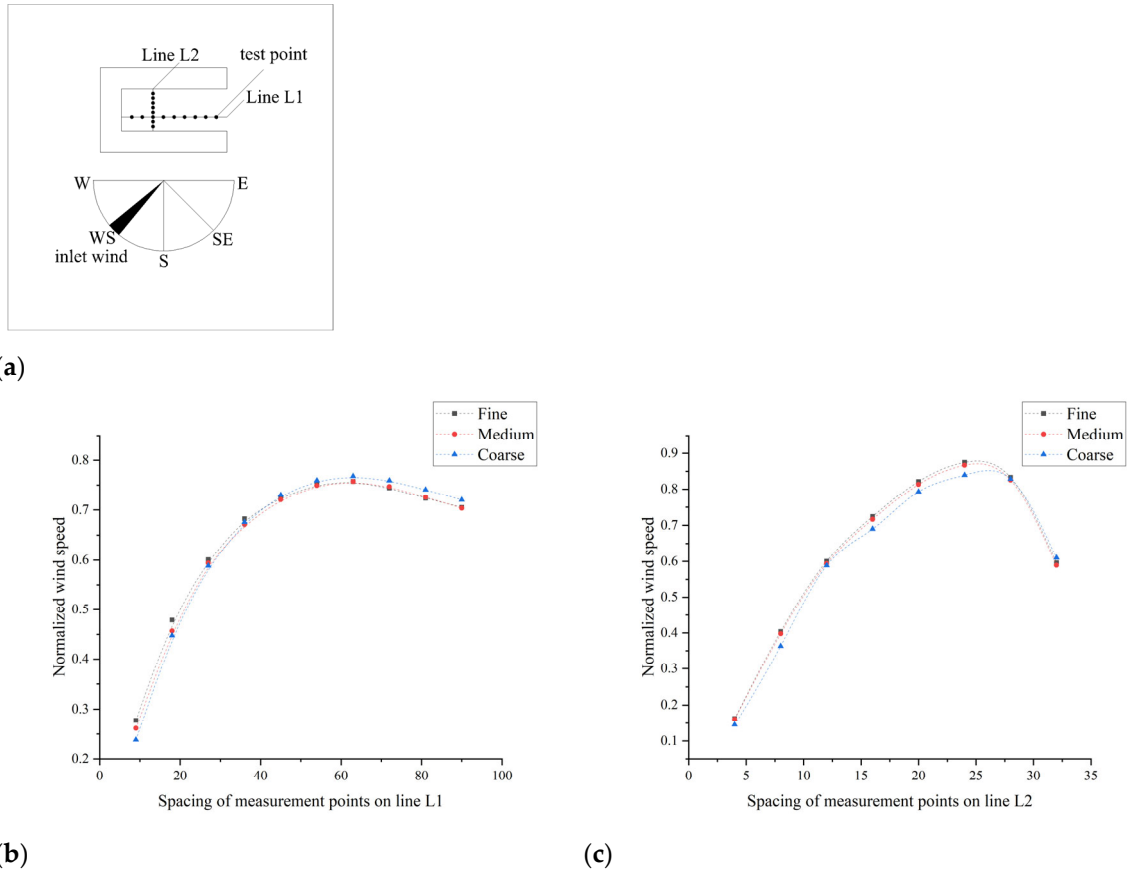

Figure 4. Grid sensitivity test. (**a**) Grid sensitivity test points. (**b**) Comparison of horizontal grid sensitivity. (**c**) Comparison of vertical grid sensitivity.

2.5. Simulation Validation

A CFD validation process was performed to ensure the credibility of the final results. This study uses Zhejiang University of Science and Technology's teaching building No. 2 as a research prototype, which is a U-shaped building with an enclosed internal courtyard open on the east side and an elevated design in the center of the south and north buildings, as shown in Figure 5b. During the CFD validation process, the courtyard of the teaching building was selected as the field measurement location. Field measurements were taken at 7 locations in the courtyard using a high-precision anemometer—the Kestrel 5500—throughout 20 October 2022, from 9:00 a.m. to 10:00 p.m., with wind speeds recorded every 2 s. Figure 5a shows the locations of all measurement points. Six measurement points are located in the courtyard:

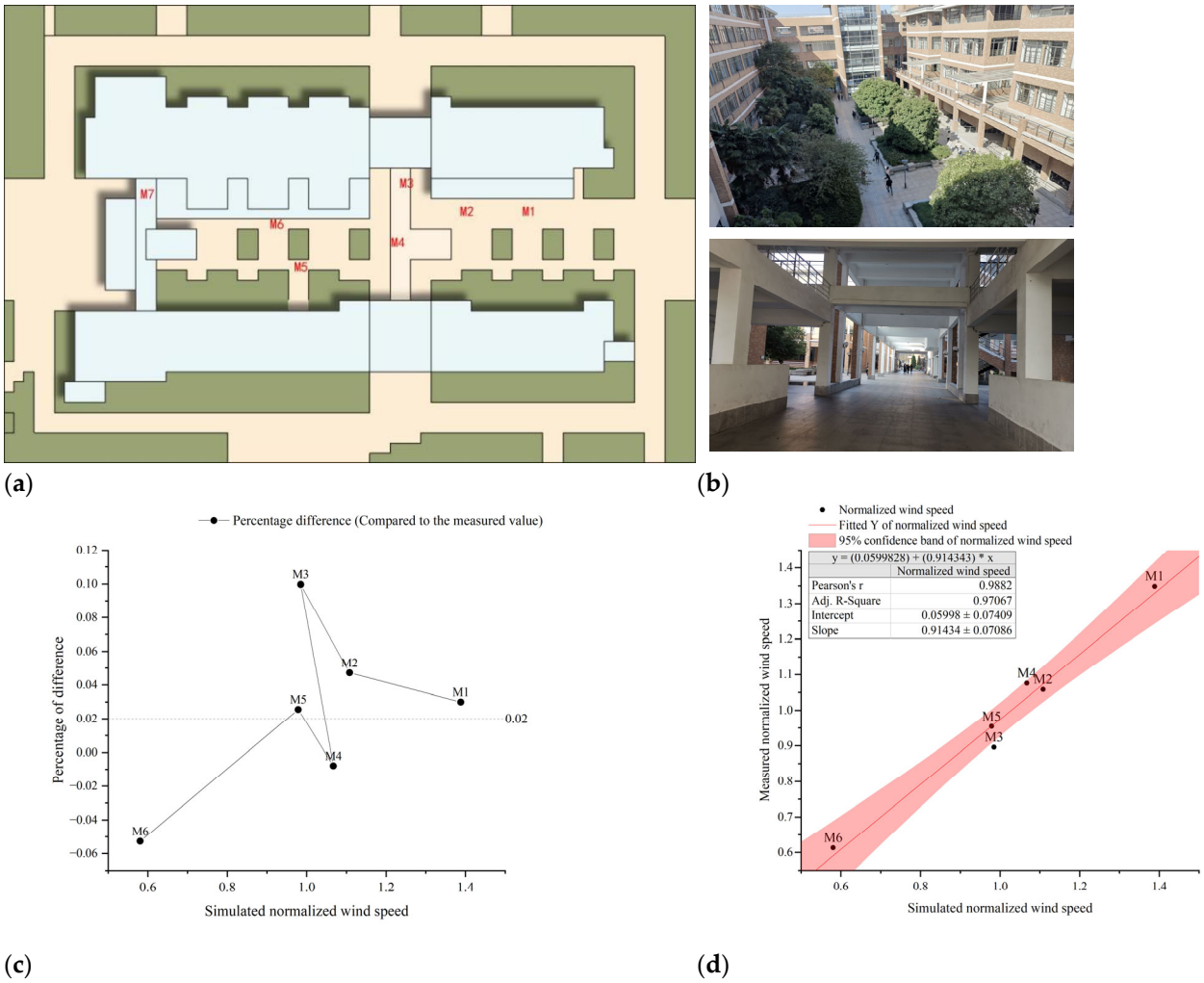

Figure 5. Simulated verification. (**a**) On-site measurement point of No. 2 teaching building of Zhejiang Sci-Tech University. (**b**) On-site measurements of academic building courtyards and overhead areas. (**c**) Rates of change in simulated values of normalized wind speed at each measurement point relative to the measured values. (**d**) Fitting equations for simulated and measured wind speed.

M1 and M2 are in the eastern part of the courtyard.

M3 is on the elevated ground floor of the courtyard to reflect the airflow in the elevated area.

M4 is in the middle of the connecting corridor.

M6 is in the western part of the courtyard.

M5 is in the middle of the courtyard to reflect the airflow in the center.

An additional measurement point, M7, is located on the roof at a height of 20 m to measure the reference wind speed (U_{ref}) and wind direction. Ground measurement spots were placed at 1.8 m above ground level to evaluate the wind conditions at pedestrian heights. The simulated experiment used the CFD method for the identical scenario as the on-site measurement. A simplified model was created based on the actual shape of the No. 2 teaching building, and numerical simulation was performed using the grid division and boundary constraints mentioned in the previous section. The wind speed and direction under the boundary conditions are derived from meteorological data collected between 9 a.m. and 10 p.m. The wind's plural direction is 90 degrees east, with an average wind speed of 3.41 m/s. Wind speeds at 7 locations were recorded and compared between simulated and field measurements. The standardized wind speed represents the simulation precision for improved validation. The following equation defines the standardized wind speed:

$$U_N = U/U_{ref} \quad (8)$$

where U_N is the standardized wind speed, U is the wind speed at the courtyard measurement point, and U_{ref} is the wind speed at the roof measurement point M7. The measured and simulated averages for one day were normalized to verify the error between the field measurements and the simulated results. Figure 5c displays the % difference in simulated wind speed compared to measured wind speed at locations M1 to M6 for the same initial wind direction. The simulation method accurately replicated the field observations, with an average variance of 2%. The largest deviation value is around 10% at position M3 due to its location near the border of the columns at the overhead, where the airflow field is unstable. Most of the measured standardized wind speeds are smaller than the simulated wind speeds because the model used in the simulation experiments was simplified and ignored the influence of details such as foot traffic and vegetation on reducing the wind speed. Figure 5d displays a linear regression comparing the measured and simulated values. The linear regression equation is y = 0.06 + 0.91x. The correlation coefficient (Pearson's r) is 0.99, and the adjusted coefficient of determination (Adj. R-Square) is 0.97, indicating a strong fit between the measured and simulated values. The PHOENICS simulated wind speed figures closely align with the measured wind speed readings in the field. The PHOENICS settings and boundary conditions are appropriate for modeling the wind conditions in the courtyard. The grid layout and boundary condition settings outlined in the previous section will be maintained for additional analysis.

3. Statistical Results

3.1. Wind Environment Indicators for the No-Elevation Program Courtyard

Figure 6 displays the wind environment indicators of the courtyard space in the academic building for three wind directions without overhead constructions. The MV (1.33 m/s) and Vσ (0.44 m/s) are the highest in the courtyard when the wind blows from the southwest. Conversely, the MV (0.73 m/s) and Vσ (0.24 m/s) are the lowest in the courtyard when the wind comes from the south. The average MV of the courtyard for the no elevation plan is 1.10 m/s under all three wind directions, while the average Vσ is 0.34 m/s. The MA (266 s) and Aσ (29 s) of courtyards under the SE wind direction were the lowest, while the MA (351 s) and Aσ (84 s) of courtyards under the S wind direction were the highest. In the no-elevation situation with three wind directions, the mean MA of the courtyards is 303 s, whereas the average Aσ is 43 s.

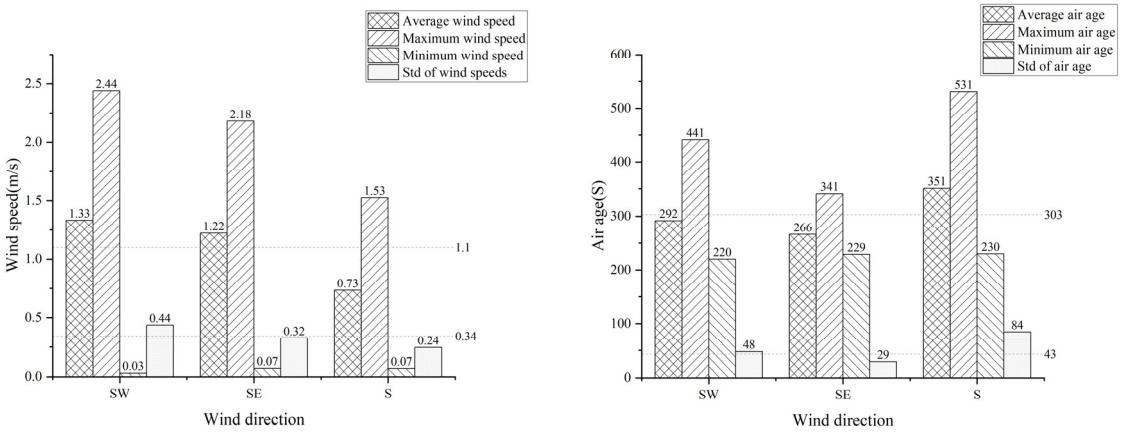

(**a**) (**b**)

Figure 6. Wind environment indicators for the courtyard of the non-elevated scheme. (**a**) Mean wind speed and standard deviation of wind speed. (**b**) Mean air age and standard deviation of air age.

3.2. Overall Effect of Elevation on the MV

3.2.1. Comparison of the MV

Figures 7a and 8a illustrate that out of the 93 elevated design cases, 50 elevation designs resulted in yard mean wind speeds lower than those in the un-elevation scenario (V = 1.10 m/s). Over half of the elevation scenarios experienced decreasing yard mean wind speeds, with a median of 1.07 m/s, a mean of 1.03 m/s, and a standard deviation of 0.22 m/s. The data followed a normal distribution (K-S test, $p = 0.10$), and a one-sample *t*-test indicated that the MV of the courtyard with the elevation design ($n = 93$, mean = 1.03 m/s) was significantly lower than that of the un-elevated scheme (V = 1.10 m/s) ($p = 0.003 < 0.01$), as depicted in Figure 9a. Overall, elevation led to a significant decrease in average yard wind speed ($p < 0.01$).

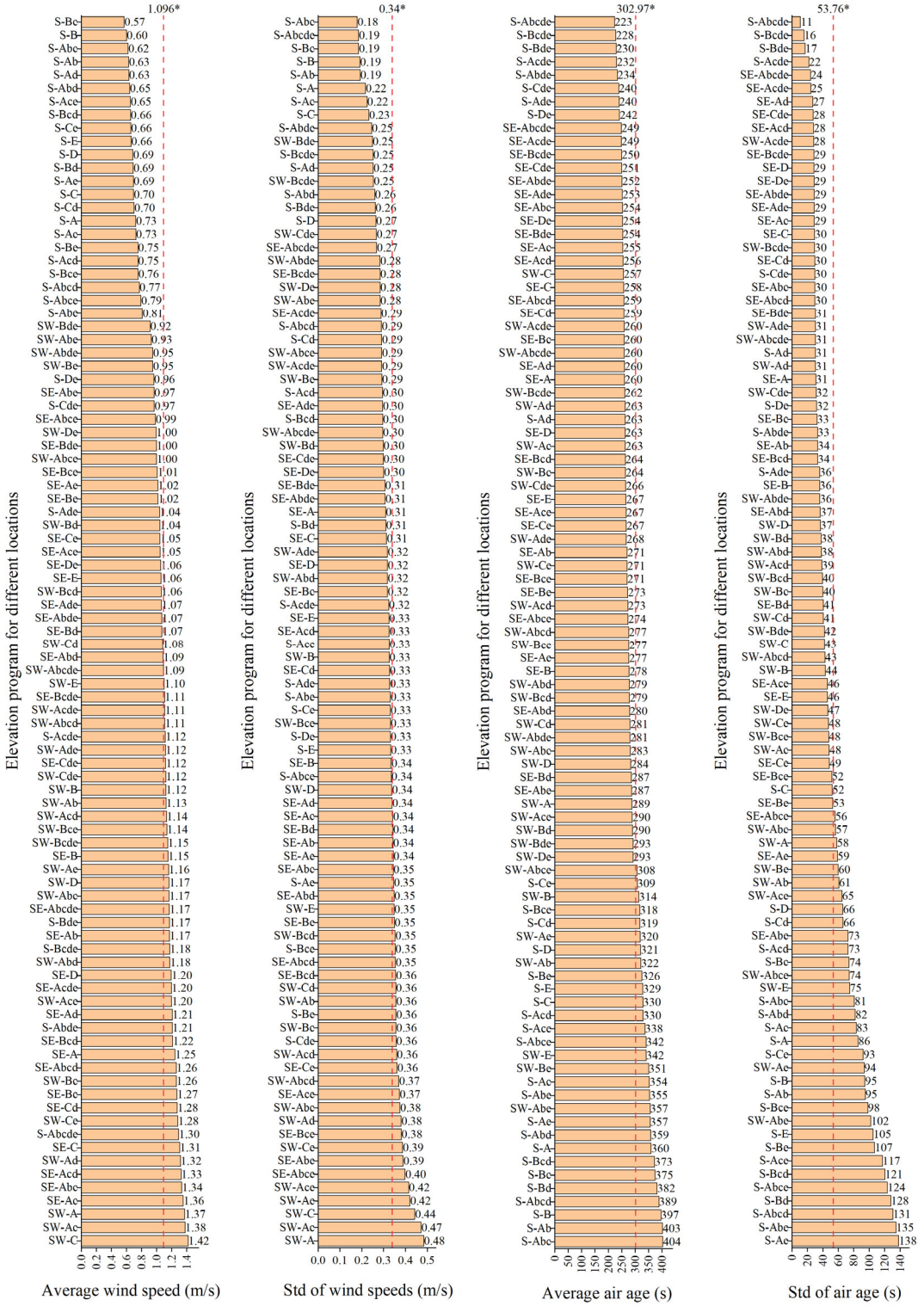

Figure 7. Bar chart of wind environment indicators for the courtyard of the elevated scheme. (**a**) Bar chart of average wind speed. (**b**) Bar chart of standard deviations of wind speed. (**c**) Bar chart of average air age. (**d**) Bar chart of standard deviation of air age. * Unelevated scheme.

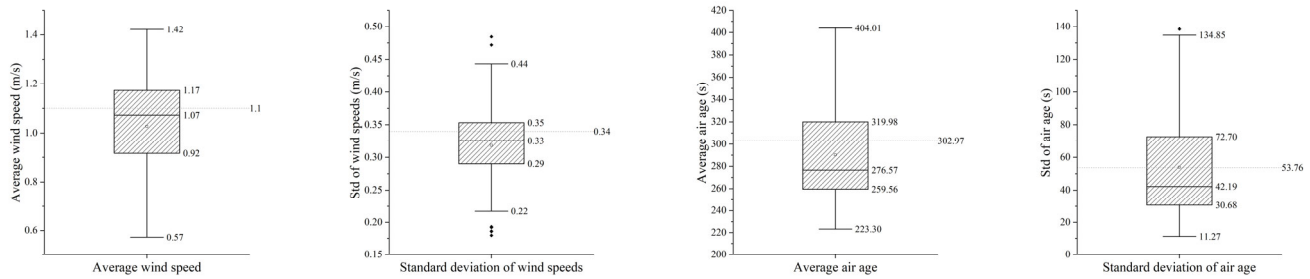

(**a**) (**b**) (**c**) (**d**)

Figure 8. Box line diagram of wind environment indicators for the courtyard of the elevation scheme. (**a**) Average wind speed. (**b**) Standard deviation of wind speed. (**c**) Average air age. (**d**) Air age standard deviation.

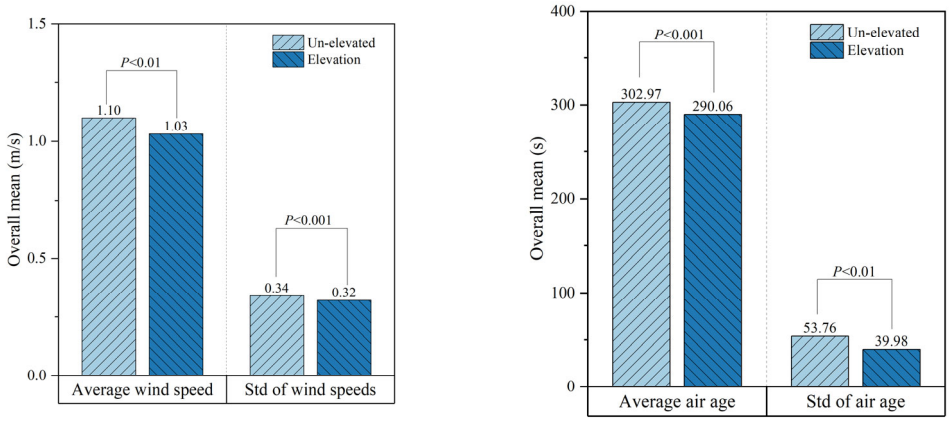

(**a**) (**b**)

Figure 9. Comparison of mean values of wind environment indicators for elevation and no-elevation scenarios. (**a**) Wind speed-related indicators. (**b**) Air age-related indicators.

3.2.2. Effect of Elevation at Different Locations on the MV

The mean value of ΔMV (ΔMV_{mean}) data for the two levels (i.e., non-elevated and elevated groups) for each of the five elevated location factors was normally distributed with consistent variation after removing extreme outliers. The analysis of variance revealed that the ΔMV_{mean} produced by the A, B, C, and D position factors at different levels of elevation and no elevation were not significantly different, as shown in Figure 10a. Location E in the overhead case had a ΔMV_{mean} of −0.13, which is significantly smaller ($p < 0.001$) than the ΔMV_{mean} of −0.06 in the no overhead case.

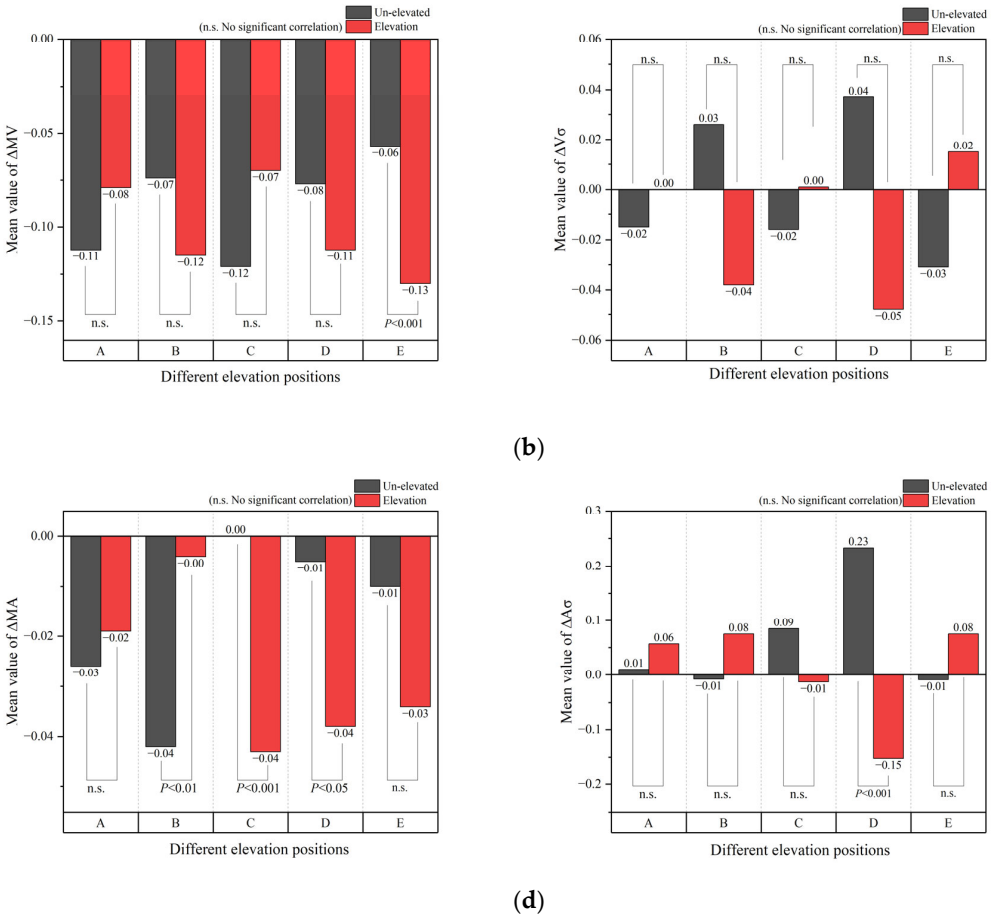

Figure 10. Comparison of the difference between the location being elevated or not on the mean value of the rate of change for the wind environment indicator. (**a**) Rate of change in mean wind speed. (**b**) Rate of change in the standard deviation of wind speed. (**c**) Rate of change in mean air age. (**d**) Rate of change in the standard deviation of air age.

3.3. Overall Effect of Elevation on the Vσ

3.3.1. Comparison of the Vσ

Figures 7b and 8b demonstrate that out of the 93 elevation design scenarios, 60 resulted in a Vσ lower than the non-elevation scheme (Vσ = 0.34 m/s). Over half of the overhead schemes experienced a decrease in Vσ, with a median of 0.33 m/s, a mean of 0.32 m/s, and a standard deviation of 0.06 m/s. After excluding outliers, the Vσ data for all elevated design cases follow a normal distribution (K-S test, $p = 0.20$). Figure 9a shows that the mean Vσ for all elevation schemes ($n = 93$, $V\sigma_{mean} = 0.32$ m/s) was significantly lower than that of the un-elevation scheme (Vσ = 0.34 m/s) based on a one-sample *t*-test ($p < 0.001$). Elevation significantly decreases Vσ in the courtyard ($p < 0.001$) and improves wind speed homogeneity.

3.3.2. Effect of Elevation at Different Locations on the Vσ

The ΔVσ data for the two levels of the five overhead location variables, the no overhead group and the overhead group exhibit normal distribution and equal variance. An ANOVA analysis indicated that the mean values of ΔVσ produced by the five location factors, with and without overhead at various levels, were not statistically different; as illustrated in Figure 10b. There was no significant difference in the rate of change in yard wind speed homogeneity among the five locations, whether elevated or not.

3.4. Overall Effect of Elevation on the MA

3.4.1. Comparison of the MA

Figures 7c and 8c show that 64 out of 93 cases of the elevation designs resulted in an MA lower than that of the un-elevation scheme (302.97 s). Approximately 75% of the elevation schemes decreased in MA, with a median of 276.57 s, a mean of 290.06 s, and a standard deviation of 44.29 s in the dataset. The one-sample *t*-test revealed that the MA (n = 93, MA_{mean} = 290.06 s) was significantly lower ($p < 0.01$) following the elevation design compared to the un-elevated scheme, as depicted in Figure 9b. Elevation significantly reduces the MA, promoting ventilation and the influx of fresh air.

3.4.2. Effect of Elevation at Different Locations on the MA

The ΔMA data exhibited a normal distribution with identical variation in both the non-elevated and elevated groups of the five elevated location components. ANOVA showed that the ΔMA_{mean} values from locations B, C, and D were significantly different at both elevation levels after removing any confounding factors. The ΔMA_{mean} values from locations A and E were not significantly different, as shown in Figure 10c. A significant increase ($p = 0.01 < 0.01$) in ΔMA was observed in position B elevated ($\Delta MA_{mean} = -0.002$) compared to not elevated ($\Delta MA_{mean} = -0.04$); a significant decrease ($p = 0.004 < 0.001$) in ΔMA was observed in position C elevated ($\Delta MA_{mean} = -0.04$) compared to not elevated ($\Delta MA_{mean} = -0.002$); and a significant decrease ($p < 0.05$) in ΔMA was observed in position D elevated ($\Delta MA_{mean} = -0.04$) compared to not elevated ($\Delta MA_{mean} = 0.01$).

3.5. Overall Effect of Elevation on the Aσ

3.5.1. Comparison of the Aσ

Among the 93 raised design situations, 60 elevation schemes had a lower Aσ value compared to the un-elevation scheme (Aσ = 53.76), as depicted in Figures 7d and 8d. The Aσ for the >1/2 overhead scheme is decreased, with a median of 42.19 s, a mean of 53.91 s, and a standard deviation of 30.86 s for the data. The data showed a non-normal distribution. The median of the overall Aσ for the elevation design scheme ($A\sigma_{med}$ = 39.98) was significantly lower than that of the un-elevation scheme (Aσ = 53.76) based on the one-sample rank-sum test ($p < 0.01$), as shown in Figure 9b. The elevation benefits the homogeneity of the air age of the courtyard.

3.5.2. Effect of Elevation at Different Locations on the Aσ

The data exhibited a normal distribution with equal variation in the no-elevated and elevated groups of the ΔAσ for each of the five elevated location factors. ANOVA analysis showed that location D had significantly different $\Delta A\sigma_{mean}$ at the two levels of elevation and no elevation after excluding confounding, as depicted in Figure 10d. Location D with elevation had a significantly lower $\Delta A\sigma_{mean}$ of −0.15 than $\Delta A\sigma_{mean}$ of 0.23 without elevation ($p < 0.001$). The difference in $\Delta A\sigma_{mean}$ between elevated and non-elevated locations A, B, C, and E is not statistically significant.

3.6. Correlation of Wind Environmental Indicator Factors

For 93 elevation design cases, after excluding extreme outliers, the four wind environment indicator factors of ΔMV, ΔVσ, ΔMA, and ΔAσ are not all normally distributed. Spearman's correlation analysis was conducted on the wind environment index factors, as presented in Table 3 and Figure 11; the following conclusions was made: The ΔMV and the ΔVσ are significantly associated with a medium correlation coefficient of 0.637 ($p < 0.001$). The ΔMV is negatively correlated with the ΔMA, with a low correlation coefficient of −0.364 ($p < 0.001$). There is no significant association between the ΔMV and the ΔAσ. The ΔVσ is positively connected with the ΔAσ (r = 0.340, $p < 0.001$), indicating a low association. The ΔVσ is not significantly correlated with the ΔMA. The ΔMA and the ΔAσ are significantly positively correlated (r = 0.683, $p < 0.001$), indicating a moderate correlation.

Table 3. Correlation matrix of wind environmental factors (Spearman's correlation).

	ΔMV	ΔVσ	ΔMA
ΔVσ	0.637 **		
ΔMA	−0.364 **	−0.128	
ΔAσ	−0.084	0.340 **	0.683 **

** At the 0.01 level (two-tailed), the correlation is significant.

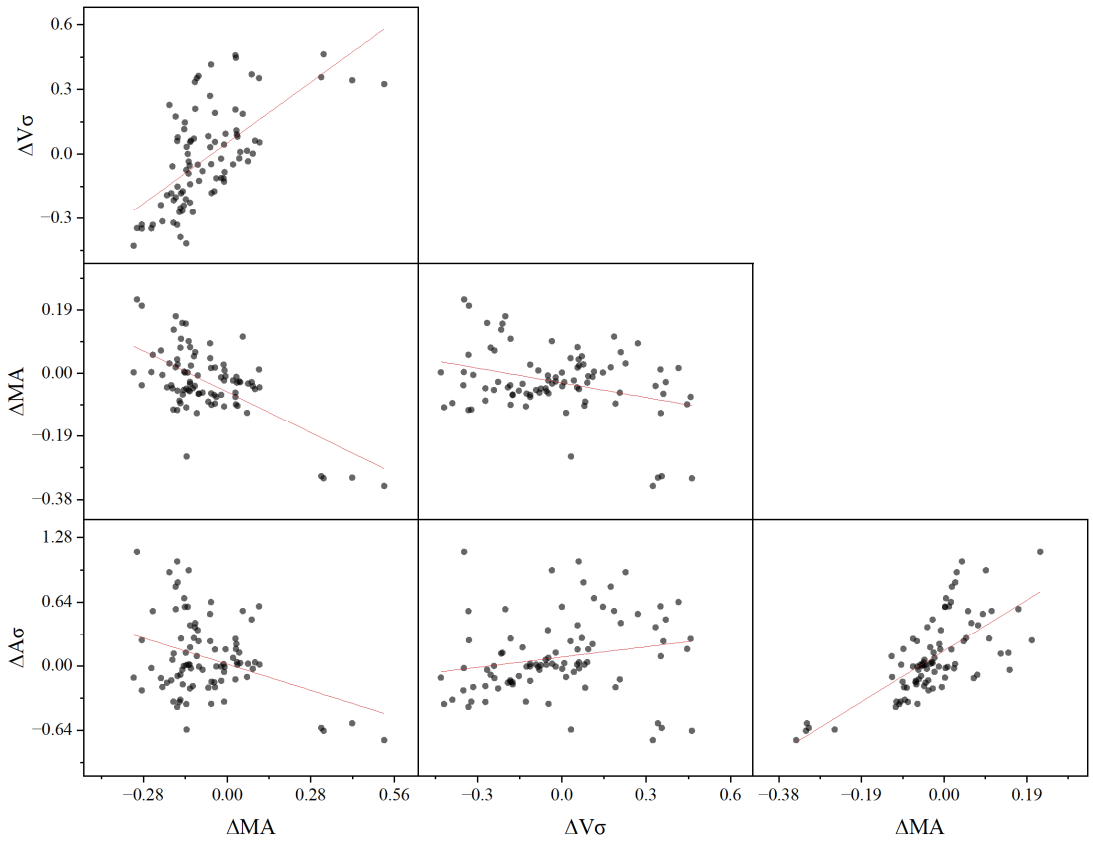

Figure 11. Scatterplot matrix of wind environmental factors.

4. Analysis and Discussion

4.1. Wind Environment Analysis of the Courtyard for the Un-Elevated Scenario

Figure 12 shows that in the un-elevation scheme, airflow in the courtyard primarily comes in through the eastern opening and the top. Some of the entering airflow is obstructed by the buildings around the courtyard, causing it to flow back into the courtyard's interior. A low-wind vortex zone is formed in areas close to buildings in Areas III and IV of the courtyard under the SW wind, with lower wind speed and higher air age. While areas near buildings and courtyard openings in Area II undergo higher wind speed and lower air age. Inside the courtyard, the wind speed decreases steadily from northeast to southwest, while the air age increases accordingly; as shown in Figure 12a. When the approaching wind is SE, due to the obstruction of the building's E location, a greater wind shadow area is generated in courtyard IV, especially in the area of IV near the building, where the wind speed is lower, and the air age is greater. The northern section of the courtyard against the building and courtyard IV against the opening experience higher wind speed and lower air age (see Figure 12b). When the wind comes from the south, it primarily enters through the eastern opening due to the large windward surface area. That creates a high-speed wind zone with fresh air in courtyard II, while courtyard I and III experience a large area of low wind speed with stagnant air, as shown in Figure 12c. Therefore, the choice of elevated location should be based on the wind environment pattern of the un-elevated courtyard.

The elevated position can enhance the wind conditions in the courtyard, increasing wind speed, reducing air stagnation, and improving ventilation homogeneity.

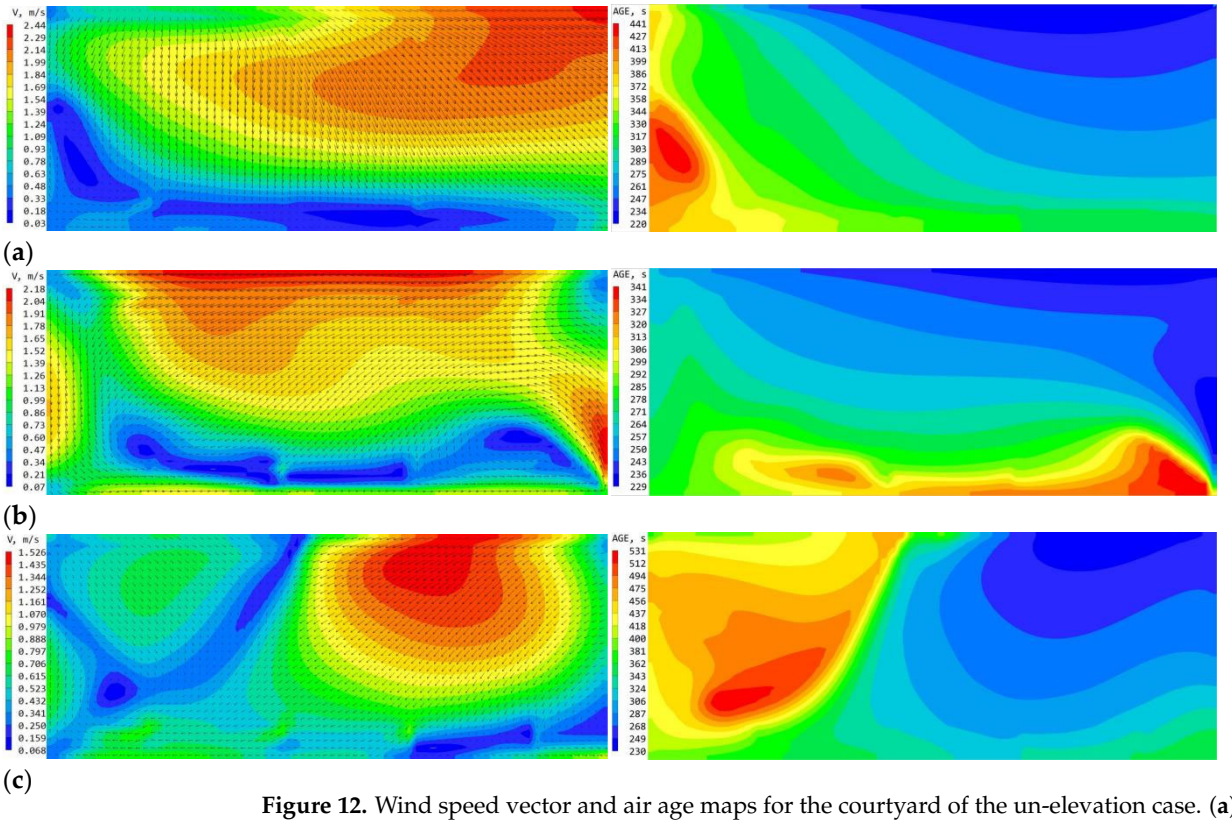

Figure 12. Wind speed vector and air age maps for the courtyard of the un-elevation case. (**a**) Under the SW wind. (**b**) Under the SE wind. (**c**) Under the S wind.

4.2. Impact of Different Locations of Elevation on Wind Environment Indicators of the Courtyard

4.2.1. Impact of the Position A Elevation on Wind Environment Indicators

The A position, elevated or not, has no significant impact on the courtyard's wind environment. This is primarily because while a position elevated on the ground floor increases airflow inflow and outflow, the A position is far away from the approaching wind direction, resulting in less airflow in and out of A. Thus, it has minimal impact on wind speed and air age. Airflow changes can be observed in the single A position elevation, as depicted in Figures 13a and 14. The MV and the MA do not change much under all three wind directions. Under SW wind, part of the airflow into the courtyard flows out of position A elevation, increasing wind speed in the I area. The Vσ ($\Delta V\sigma = 0.11$) and the Aσ ($\Delta A\sigma = 0.22$) are both increased. Under SE wind, air flows directly out of elevation A, increasing wind speed, decreasing air age, and slightly increasing Vσ ($\Delta V\sigma = 0.08$) in courtyard area I. With a S wind, part of the airflow bypasses the building and enters the courtyard from A, raising the wind speed in the I area and reducing the Vσ ($\Delta V\sigma = -0.11$).

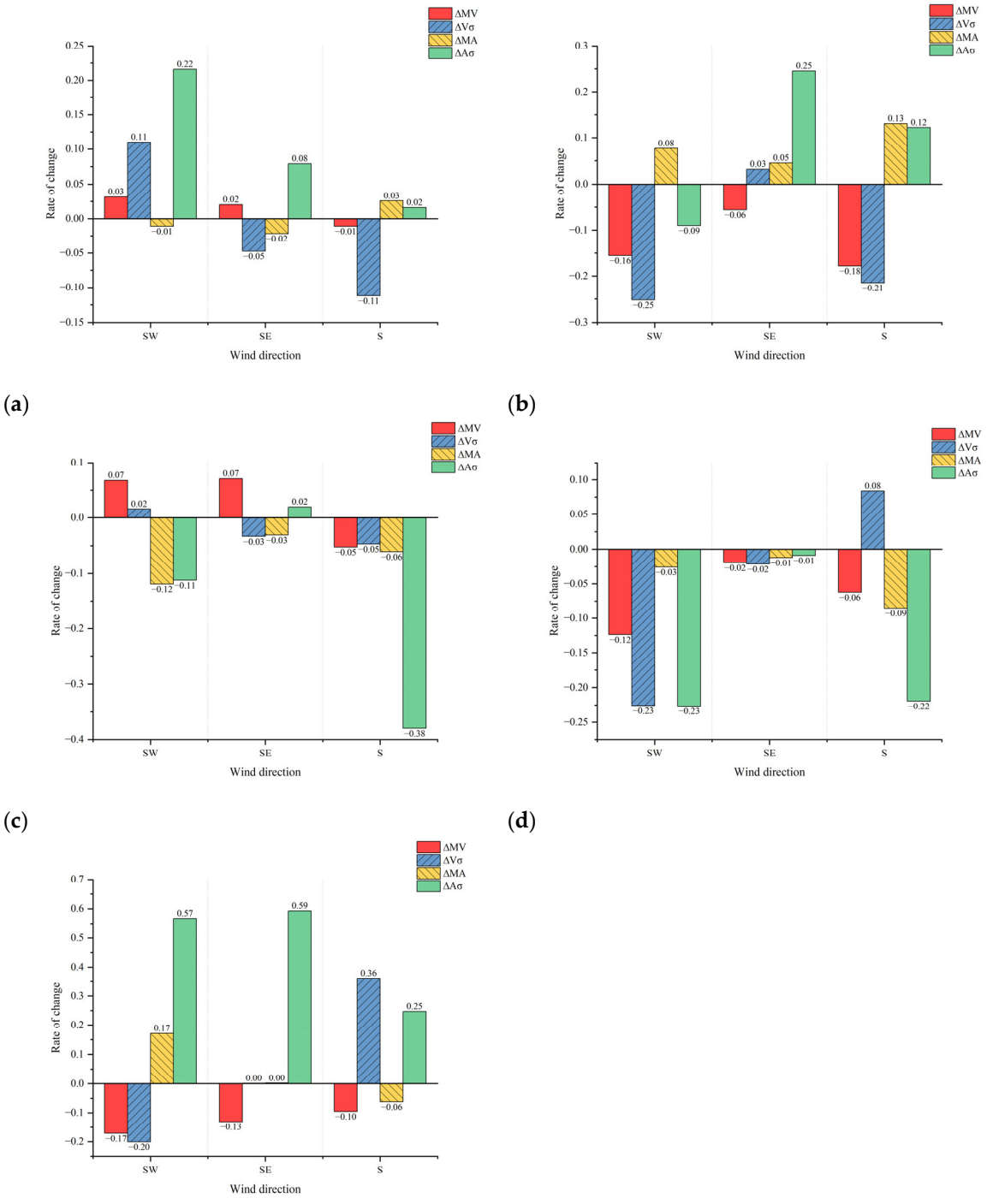

Figure 13. Histogram of wind environment indicators for courtyards with different locations of elevation. (**a**) Position A elevation. (**b**) Position B elevation. (**c**) Position C elevation. (**d**) Position D elevation. (**e**) Position E elevation.

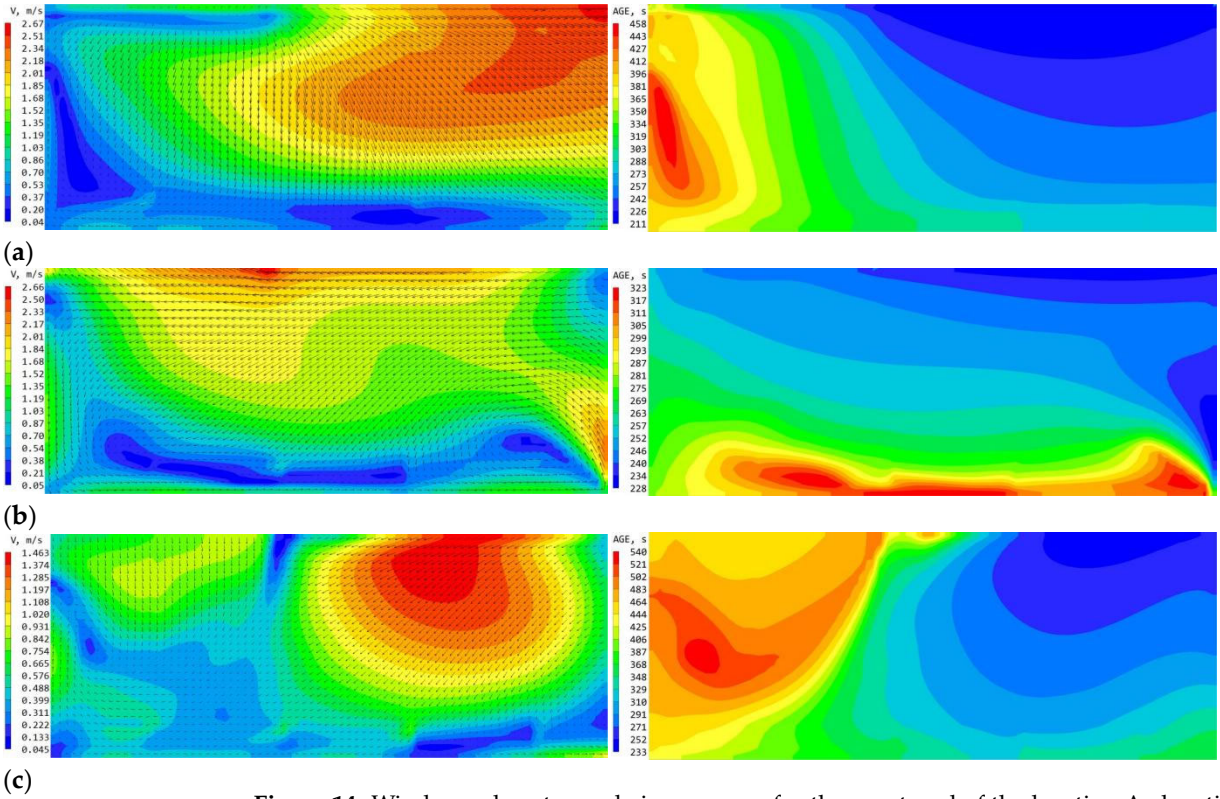

Figure 14. Wind speed vector and air age maps for the courtyard of the location A elevation case. (**a**) Location SW-A elevation case. (**b**) Location SE-A elevation case. (**c**) Location S-A elevation case.

4.2.2. Impact of the Position B Elevation on Wind Environment Indicators

While the statistical results of this study found that the BGFE significantly reduced the MA ($p < 0.001$), the opposite result was obtained for location B elevated, which significantly increased courtyard air age ($p < 0.05$). The main reason is that the elevated B position does not increase the airflow to increase the low wind speed in the southwest part of the courtyard. Instead, due to the absence of the B position on the ground floor of the building, the airflow lacks the blocking bounce of the building wall. Some airflow leaks from position B, leading to decreased airflow circulating back into the courtyard, reduced wind speed, and increased average air age. Airflow changes can be observed in the single B position elevation, as depicted in Figures 13b and 15. The MV falls, and the MA increases under all three wind directions. Under the SW wind, some airflow into the courtyard escapes from location B. The wind speed in courtyard II decreases, resulting in a decrease in the MV ($\Delta MV = -0.16$), an increase in the MA ($\Delta A = 0.08$), and a corresponding decrease in the Vσ ($\Delta V\sigma = -0.25$) and the Aσ ($\Delta A\sigma = -0.09$). Under the SE wind, the B elevation forms a straight-through airflow, which creates a wind shadow area in the courtyard IV region, with a decrease in the MV ($\Delta MV = -0.06$), an increase in the MA ($\Delta MA = 0.05$), and a large elevation in the Aσ ($\Delta A\sigma = 0.25$). Under the S wind, the courtyard III region creates a large area of low-wind vortex area, which results in the courtyard's MV ($\Delta MV = -0.18$) and Vσ ($\Delta V\sigma = -0.21$) decreased, and both the MA ($\Delta MA = 0.13$) and the Aσ ($\Delta A\sigma = 0.12$) increased.

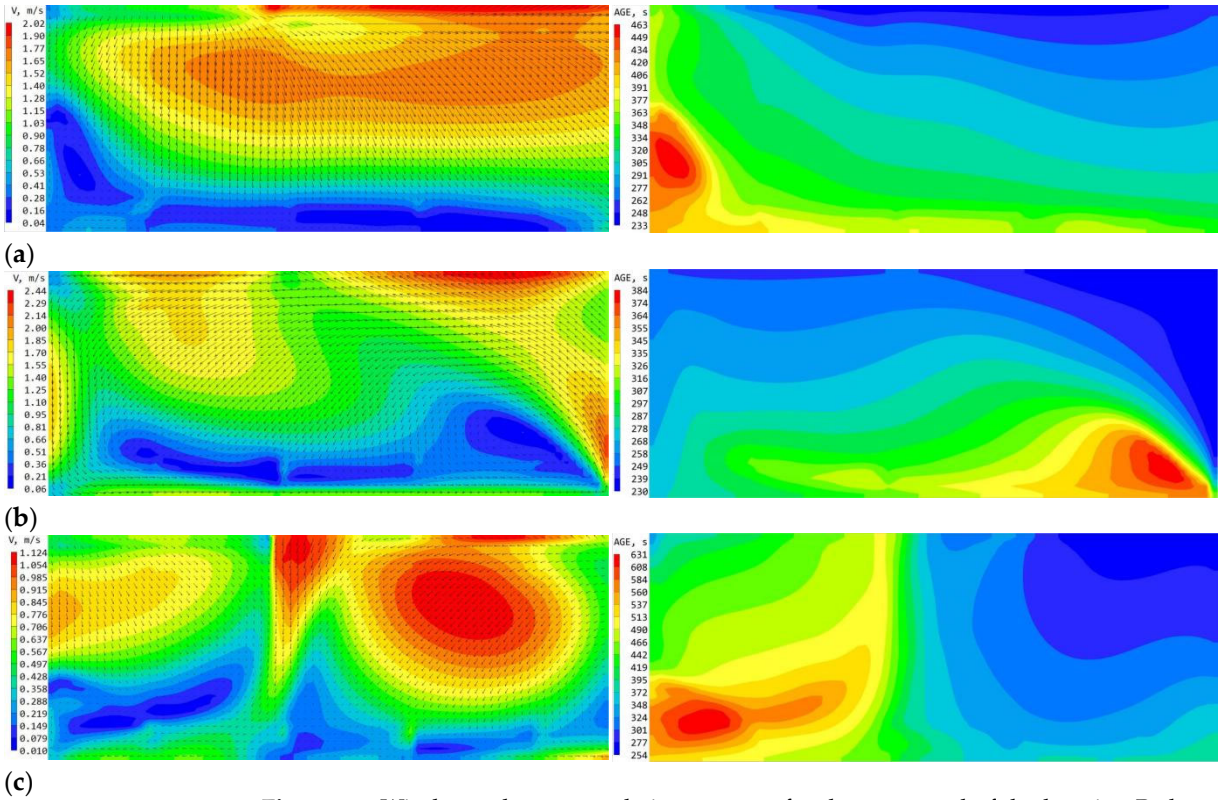

Figure 15. Wind speed vector and air age maps for the courtyard of the location B elevation case. (**a**) Location SW-B elevation case. (**b**) Location SE-B elevation case. (**c**) Location S-B elevation case.

4.2.3. Impact of the Position C Elevation on Wind Environment Indicators

The statistical analysis shows that the C position elevation significantly decreases air age ($p < 0.001$). The elevation of position C creates an east–west airflow channel. The airflow from the east or west is constricted by the buildings to the south and north of the courtyard, leading to a tight tube effect, increased airflow velocity, and a significant reduction in air age. Airflow alterations can be observed in Figures 13c and 16 in the single C position elevation. The MA decreases under all three wind directions. Under the SW wind, the building wall squeezes most of the airflow after entering straight from position C elevation, increasing the MV ($\Delta MV = 0.07$), and significantly decreasing the MA ($\Delta MA = -0.12$) and Aσ ($\Delta A\sigma = -0.11$). With the SE wind, the airflow flows out of the C position elevation, creating a penetrating wind, and resulting in an increase in the MV ($\Delta MV = 0.07$) and a slight decrease in the MA ($\Delta MA = -0.03$). With the S wind, the front of the building blocks the airflow, but some of it enters through the C position elevation. That improves ventilation of the western portion of the courtyard, with a decrease in the MA ($\Delta MA = -0.06$) and a considerable reduction in the Aσ ($\Delta A\sigma = -0.38$).

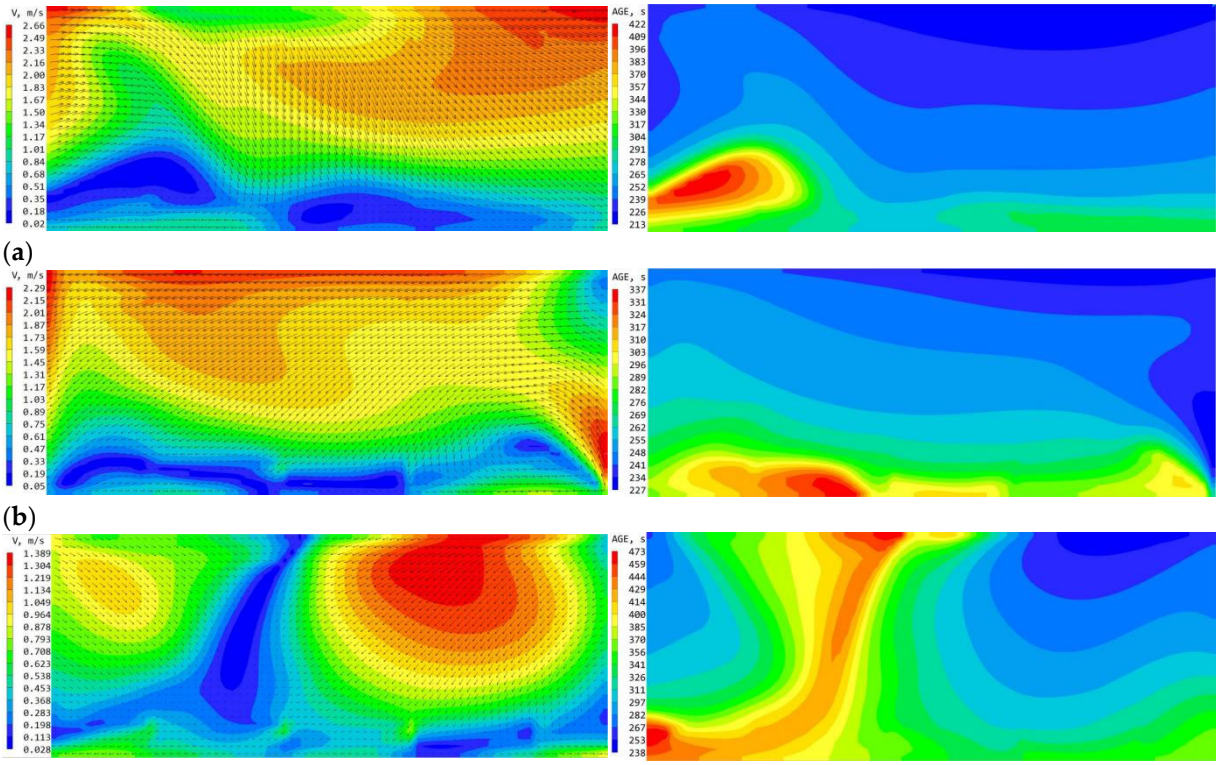

Figure 16. Wind speed vector and air age maps for the courtyard of the location C elevation case. (**a**) Location SW-C elevation case. (**b**) Location SE-C elevation case. (**c**) Location S-C elevation case.

4.2.4. Impact of the Position D elevation on Wind Environment Indicators

According to the statistical results, D position elevation significantly ($p < 0.001$) reduces air age and standard deviation compared to no elevation. The main reason is that location D is immediately adjacent to area III of the courtyard, which has the highest air age and the worst ventilation. Thus, regardless of the wind direction, the elevation of position D induces airflow to enter from position D, enhancing ventilation in the poorly ventilated western section of the courtyard, leading to decreased air age in that area and lowering the Aσ. Airflow changes can be seen at the single D position elevation, as shown in Figures 13d and 17. The MA and Aσ decrease for all three wind directions. Under the SW wind, the airflow enters directly from elevation D, improving courtyard III's ventilation. Due to the compression effect of the airflow, a larger wind shadow area forms in the courtyard's center. This results in a decrease in the MV (ΔMV = −0.12), a slight decrease in the MA (ΔMA = −0.03), and significant decreases in the Vσ (ΔVσ = −0.23) and the Aσ (ΔAσ = −0.23). Under the SE wind, less airflow enters the courtyard from position D, improving the wind environment in courtyard III with a slight decrease in the MA (ΔMA = −0.01). Under the S wind, airflow enters the courtyard straight from position D elevation, increasing the wind speed. That causes a decrease in the MA (ΔMA = −0.09) and Aσ (ΔAσ = −0.22). However, it produces a larger wind shadow area in courtyard IV, resulting in a lower MV (ΔMV = −0.06) and higher Vσ (ΔVσ = 0.08).

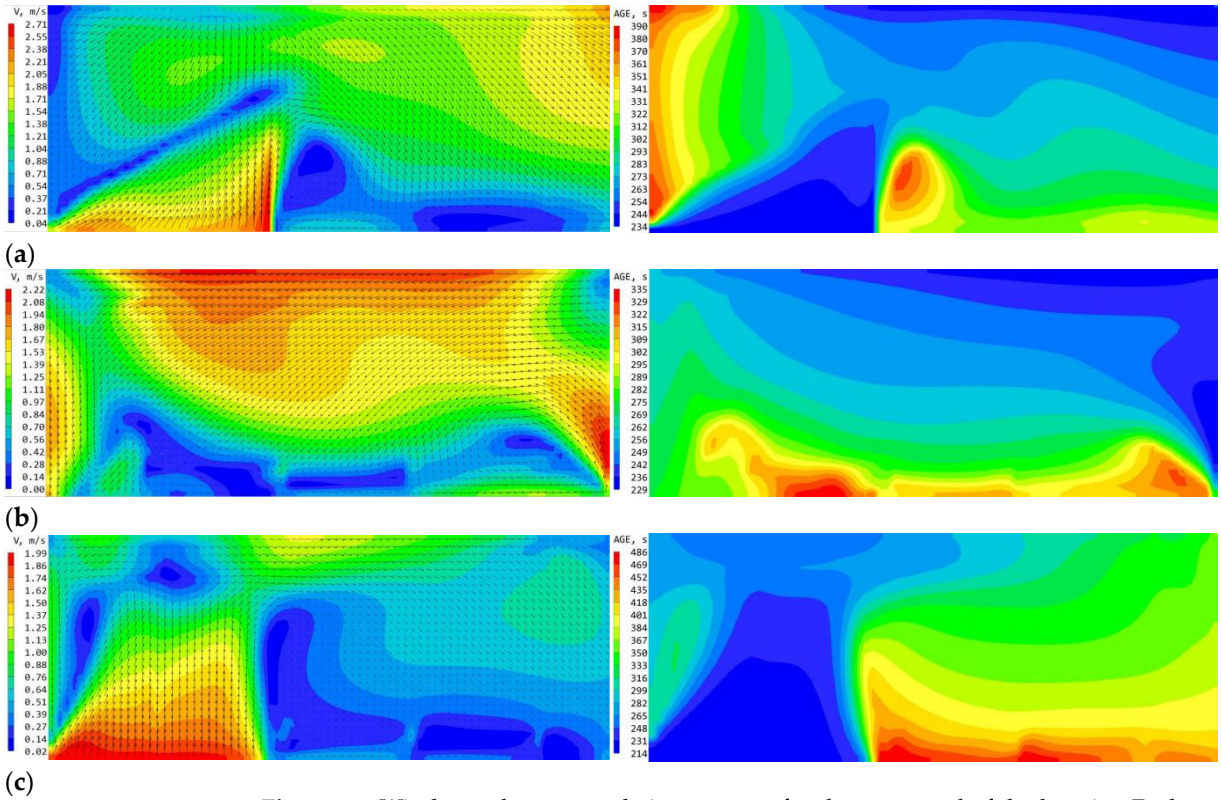

Figure 17. Wind speed vector and air age maps for the courtyard of the location D elevation case. (**a**) Location SW-D elevation case. (**b**) Location SE-D elevation case. (**c**) Location S-D elevation case.

4.2.5. Impact of the Position E Elevation on Wind Environment Indicators

According to the statistical results, the elevated E position significantly reduces the wind speed compared to no elevation ($p < 0.05$). The elevated E position results in direct airflow from the E elevated, but it does not improve the poor ventilation in the southwestern part of the courtyard. Instead, it increases the wind shadow area in courtyard III, lowering the average wind speed. Airflow changes can be seen at the single E position elevation, shown in Figures 13e and 18. The MV is reduced in all three wind directions. Under the SW wind, part of the airflow enters from the E position, creating a low wind speed zone in courtyard IV, with a decrease in MV ($\Delta MV = -0.17$) and Vσ ($\Delta V\sigma = -0.20$), an increase in MA ($\Delta MA = 0.17$), and an increase in Aσ ($\Delta A\sigma = 0.57$). Under SE wind, airflow enters from E elevation, resulting in a considerable decrease in air age in courtyard IV but forming a low wind speed vortex zone in courtyard III, reducing the MV ($\Delta MV = -0.13$) and significantly increasing the Aσ ($\Delta A\sigma = 0.59$). With the S wind, the airflow enters directly from the E position, increasing wind speed in courtyard IV. However, it creates a large area of low wind speed vortex in courtyard III, leading to a decrease in MV ($\Delta MV = -0.10$) and MA ($\Delta MA = -0.06$), but a notable increase in Vσ ($\Delta V\sigma = 0.36$) and Aσ ($\Delta A\sigma = 0.25$).

The ground-floor elevation is not always conducive to improving the air quality of the courtyard space. The main reason is that different elevation positions have different mechanisms for influencing the air age of the courtyard. Whether or not the A position is elevated does not affect the air quality of the courtyard space; the C or D position of the elevation will significantly reduce the air age of the courtyard space, which is favorable to the improvement of the air quality of the courtyard. However, the B position of the elevation will increase the air age instead, which will reduce the air quality of the courtyard space. Position E will lead to a significant reduction in wind speed inside the courtyard, thus affecting the courtyard ventilation and wind-heat comfort. Therefore, the bottom-floor elevation of the U-shaped courtyard building should pay attention to the correct selection of the elevation position, and the improper elevation position will deteriorate the wind environment of the courtyard space.

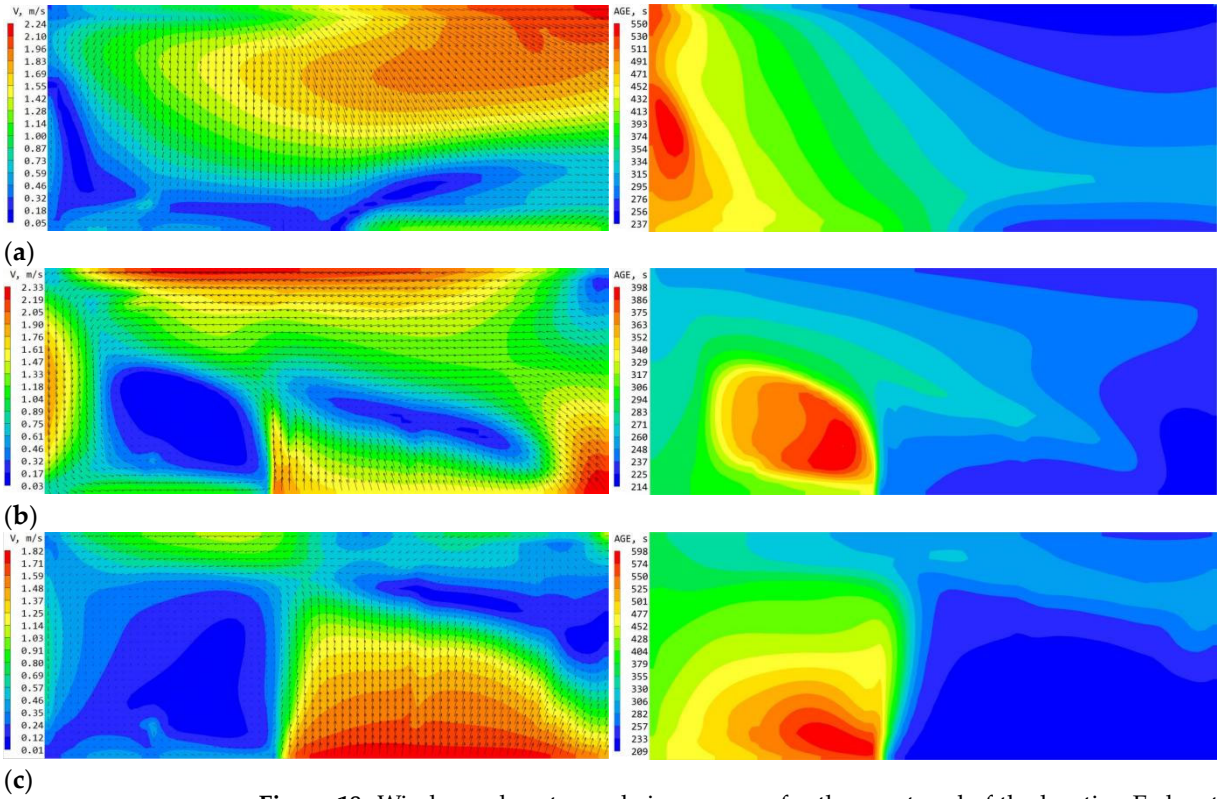

Figure 18. Wind speed vector and air age maps for the courtyard of the location E elevation case. (**a**) Location SW-E elevation case. (**b**) Location SE-E elevation case. (**c**) Location S-E elevation case.

4.3. Overall Impact of Elevation on wind Environment Indicators

4.3.1. Impact of Elevation on the MV

This study found that the elevation design significantly reduces ($p < 0.01$) the MV of the U-shaped courtyard, contrary to previous research that indicated elevation design increases the wind speed at pedestrian level near buildings [6–9,21]. The primary factor is the specific spatial arrangement of the U-shaped courtyard. Enclosed U-shaped courtyards can mitigate the wind amplification caused by elevation, as supported by Liu et al.'s study [10]. For example, elevated location E, regardless of the wind direction, creates a low-wind vortex zone in Area III (Figure 18), reducing the courtyard's MV. The BGFE of the courtyard's north building (e.g., Positions B and A), which results in the absence of the building's first-floor wall, accelerates the outward escape of the airflow and reduces the folding movement of the airflow toward the interior of the courtyard, preventing more and faster airflow from reaching the low-wind zone in the western part of the courtyard (Figures 14 and 15), resulting in a lower MV. The D position elevation on the ground floor of the building facilitates airflow entering the courtyard and interacting with architectural barriers. This interaction creates a low-wind-speed static wind zone in the middle of the courtyard, lowering the MV (Figure 17). C position elevation also provides a wind shadow zone in the S wind within the courtyard, lowering the courtyard's MV (Figure 16).

Through the elevation design, scheme SW-C has the highest average wind speed in the courtyard (MV = 1.422 m/s), while scheme S-Bc has the lowest (MV = 0.572 m/s). Position C elevation under the SW wind forms a ventilation corridor from the west to the east, accelerating the airflow, as shown in Figure 16a. The location of the BC elevation under the S wind allows the courtyard space to become a wind shadow zone for the front row of buildings with reduced wind speeds (Figure 19a). Air stagnation caused by low wind speed environments may prevent the evacuation of airborne pathogens [49,50], and weak or static winds are not conducive to urban ventilation, which can exacerbate thermal discomfort for pedestrians [51]. They are not conducive to diffusing ground heat and pollutants [39]. The elevation significantly reduces the MV in the courtyard space. It is essential to note in

the design that in weak wind climates, the BGFE of the U-shaped courtyard can create low wind speed problems, resulting in poor wind and thermal comfort and leading to problems such as contamination or viruses that do not spread quickly.

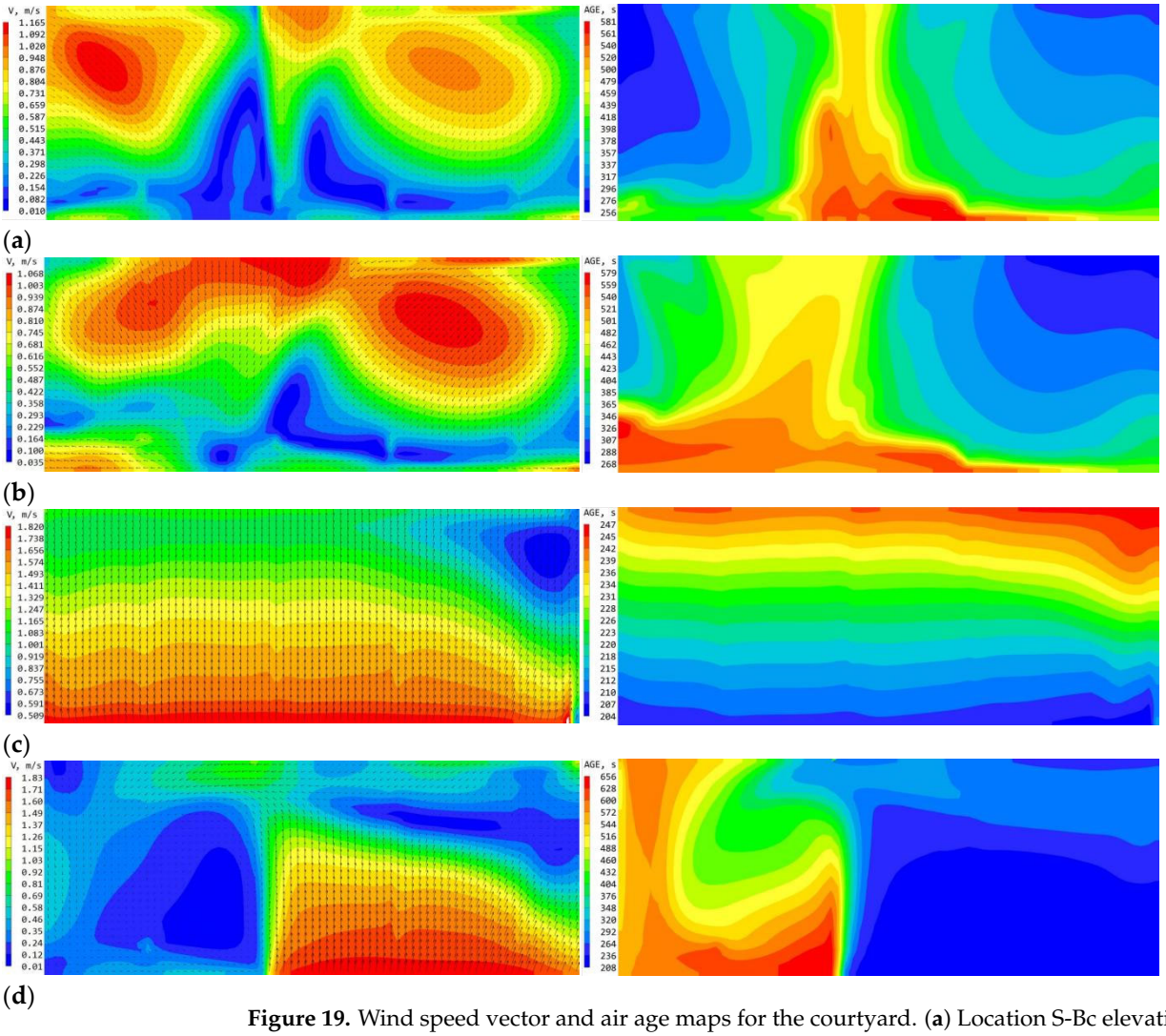

Figure 19. Wind speed vector and air age maps for the courtyard. (**a**) Location S-Bc elevation case. (**b**) Location S-Abc elevation case. (**c**) Location S-Abcde elevation case. (**d**) Location S-Ae elevation case.

4.3.2. Impact of Elevation on the MA

This study statistically found that the BGFE significantly reduced the MA ($p < 0.001$). This is in agreement with existing research results. These studies found that installing openings can improve the air exchange efficiency of courtyards [35], promote ventilation and pollutant diffusion [16,23], and introduce more fresh air [26]. In the non-elevated scheme, the southwestern location of the courtyard creates a low wind speed vortex zone, which increases the difficulty of air particles escaping the courtyard, as shown in Figure 12. The BGFE enhances airflow import and export, increasing the contact surface between the low wind speed area in the southwest courtyard and the outside air. On the other hand, the BGFE would enhance the uniformity of wind direction. Although wind speed might decrease, it will facilitate the displacement of stagnant air with fresh air in the courtyard, thus decreasing air age. For example, positions C and D, located next to the least ventilated areas in the southwestern part of the courtyard, will facilitate quicker fresh air circulation regardless of wind speed changes, thereby reducing the MA.

For the 93 elevated cases, scheme S-Abc had the highest air age (Ag = 404 s), and scheme S-Abcde had the lowest (Ag = 223 s). In the S-Abc scheme, because the front building fully limits direct air entrance to the courtyard and instead forms a wider wind

shadow zone inside the courtyard (Figure 19b), the elevated ABC position permits the airflow to escape outward. It slows circulation into the courtyard's interior, slowing the winds and increasing the age of the air. In the elevated scheme S-Abcde, the airflow becomes unobstructed by the lack of buildings at the bottom of the courtyard. The airflow path is shortest under S winds, minimizing the MA (223 s) and Aσ (11 s), as shown in Figure 19c. The BGFE is critical for reducing the air age of the courtyard space, allowing for improved air quality, and ensuring the physical and mental health of the students' activities in the courtyard. Under a public health event similar to the Coronavirus outbreak, the risk of virus transmission can be mitigated to some extent. The air quality of the courtyard space also determines the indoor air quality of the classroom [52], so the elevated design also provides a healthy air environment for students studying in the classroom, which enhances students' satisfaction with the physical environment of the building and reduces learning anxiety [37].

4.3.3. Impact of Elevation on the Aσ

Statistical analysis showed that the BGFE significantly decreased the Aσ ($p < 0.01$). Elevation exposes the courtyard interior to the outdoors, especially in the southwest section, where the air is older; minimizing the time for fresh air to circulate within and lowering the air age, thus reducing the Aσ. For example, C and D position elevation facilitates airflow to efficiently reach the least favorable ventilation regions in the courtyard, decreasing air age and the Aσ over the courtyard. Among the 93 high cases, scenario S-Abcde (Aσ = 11 s) had the lowest Aσ value. This scenario directs airflow to the long side of the courtyard in the S wind direction, resulting in better air age homogeneity throughout the courtyard in the fully elevated case (Figure 19c). The scheme S-Ae has the highest Aσ value (138 s). Due to the E position elevation, the air age of the courtyard II and IV zones falls significantly under the S wind direction. On the other hand, the E elevated position creates a wind shadow zone in courtyard III, increasing air age. Furthermore, the elevation of A permits airflow to escape and decreases airflow that folds back into the courtyard III region, resulting in a considerable rise in air age in courtyard III, eventually increasing the Aσ; as seen in Figure 19d.

4.4. Correlation between the Wind Environmental Factors

The study demonstrated a substantial negative correlation between ΔMV and ΔMA ($r = -0.364$, $p < 0.001$), supporting previous evidence [53] that higher wind speeds result in lower air age. For example, position B elevation reduces the MV and increases the MA of the courtyard in all three wind directions, indicating a negative association (Figure 13b). Position B elevation increases airflow outflow and reduces refractive airflow in the courtyard, resulting in lower MV and higher MA. However, the air age and wind velocity notably decreased in some design scenarios. The BGFE significantly decreases wind speed, whereas certain positions (e.g., sites C and D) reduce air age in the southern courtyard due to their proximity to the region's high air age, decreasing both wind speed and air age. Under SW and SE winds, C position elevation increases wind speed while decreasing air age, resulting in a negative connection, but under S winds, it decreases wind speed and air age (see Figure 13c). Elevation D reduces wind speed and air age in all three wind directions. As the airflow from site D collides with the folded back airflow, a large wind shadow area occurs in the courtyard's center, lowering the overall average wind speed. While position D is near the southwestern part of the courtyard, its elevation increases the contact surface between this location and the outside world, improving its high air age. As a result, the wind speed and air age reduce. (see Figures 13d and 17).

4.5. Limitations

This article studies elevated designs for wind directions SW, SE, and S because of space limitations; but further research is needed for additional wind directions. The article is a general statistical analysis of the data of 93 elevated design cases and lacks an in-depth

study of the respective data under different wind directions. More research is also needed into the adaptability of the BGFE in terms of thermal and wind comfort. Furthermore, the U-shaped courtyard form studied in the research is based on Zhejiang University of Technology's No. 2 teaching building as a prototype. There needs to be more research on the different wind environment effects produced by different dimensional parameters of the courtyard space, such as the height–width ratio of the courtyard form, the scale size of the courtyard, and other different courtyard forms, which need further investigation.

5. Conclusions

The article extensively investigates the impact of the BGFE on wind conditions in U-shaped courtyard spaces. After on-site measurements confirmed the correctness of the CFD simulation, 93 elevated design cases conducted numerical simulation experiments with three representative wind directions. The results were then organized and statistically analyzed. The results of the study found that the MA and Aσ of the courtyard produced by the elevated design of the U-shaped school building (MA_{mean} = 290.06 s, $A\sigma_{Med}$ = 39.98) were significantly smaller than that of the un-elevated scheme ($p < 0.01$). The MV and Vσ of wind speed of the courtyard produced by the elevated design (MV_{mean} = 1.03 m/s, $V\sigma_{mean}$ = 0.32 m/s) were significantly smaller than that of the un-overhead scheme ($p < 0.01$). It can be seen that the overhead design facilitates the arrival of fresh air and the homogeneity of ventilation but also significantly reduces the wind speed, as shown in Table 4. The correlation analysis revealed a significant negative correlation (r = −0.364, $p < 0.001$) between ΔMV and ΔMA, and a significant positive correlation (r = 0.340, $p < 0.001$) between ΔVσ and ΔAσ in the wind environment factors. There was a significant positive correlation between ΔMA and ΔAσ (r = 0.683, $p < 0.001$) and between ΔMV and ΔVσ (r = 0.637, $p < 0.001$), as indicated in Table 3. This study found that different elevation positions affect wind environment indicators differently. Position A elevated had no significant effect on the wind environment of the courtyard. Position B elevation significantly increased the MA ($p < 0.05$), position C elevation significantly decreased the MA ($p < 0.001$), position D elevation significantly increased the MA with the Aσ decreased ($p < 0.001$), and position E elevated significantly decreased the MV ($p < 0.05$), as shown in Table 5.

Table 4. Impact of the BGFE on wind environment indicators.

	MV	**Vσ**	**MA**	**Aσ**
Effects	Significant decrease	Significant decrease	Significant decrease	Significant decrease
p-value	$p < 0.01$	$p < 0.001$	$p < 0.001$	$p < 0.01$

Table 5. Impact of different elevation locations on wind environment indicators.

Rate of Change of Wind Environment Factor	**Position A**	**Position B**	**Position C**	**Position D**	**Position E**
ΔMV	N.S.	N.S.	N.S.	N.S.	S.D. ($p < 0.001$)
ΔVσ	N.S.	N.S.	N.S.	N.S.	N.S.
ΔMA	N.S.	S.I. ($p < 0.05$)	S.D. ($p < 0.001$)	S.D. ($p < 0.05$)	N.S.
Aσ	N.S.	N.S.	N.S.	S.D. ($p < 0.001$)	N.S.

N.S. No significant correlation; S.D. Significant decrease; S.I. Significant increase.

To enhance the courtyard space's ventilation and create a healthy wind environment, a strategic selection of elevation location is necessary, rather than a random design of elevation. Position E elevated is not recommended for increasing wind speed; positions C and D elevated are recommended for reducing air age and increasing ventilation, while position B elevated is not; and position D elevated is recommended for increasing air age homogeneity. Overall, elevations C and D are advised to create a healthy wind environment in the U-shaped courtyard, whereas elevations B and E are not. Although the BGFE significantly reduces the MA of the courtyard and facilitates fresh air, it also significantly

reduces the MV. It should be noted that the potential low wind speed problem associated with the BGFE, especially in weak wind climates, can lead to less diffusion of pollution or viruses and poor wind and thermal comfort. Further research is needed to explore the specifics of each wind direction in-depth and to study the impact of the BGFE on wind and thermal comfort in the courtyard space. The findings of this article have theoretical implications for the design of courtyard elevations based on the creation of a healthy wind environment, as well as the design of green renovations to existing courtyard buildings.

Author Contributions: Conceptualization, Q.W.; Methodology, H.L., Q.Z. and Q.G.; Software, H.L.; Formal analysis, Q.W.; Investigation, Q.W., P.W. and L.Z.; Resources, H.L. and Q.G.; Data curation, Q.W.; Writing—original draft, Q.W.; Writing—review & editing, Q.W., P.W. and L.Z.; Visualization, Q.W.; Supervision, Q.W., Q.Z. and Q.G.; Project administration, Q.W.; Funding acquisition, Q.Z. and Q.G. All authors have read and agreed to the published version of the manuscript.

Funding: This study was supported by the National Natural Science Foundation of China (NSFC) [32371650, 31872688] and the National Social Science Fund of China (22BGL193).

Data Availability Statement: The original contributions presented in the study are included in the article, further inquiries can be directed to the corresponding authors.

Conflicts of Interest: The authors declare that they have no known competing financial interests or personal relationships that could have appeared to influence the work reported in this paper.

References

1. Li, J.; Niu, J.; Mak, C.M.; Huang, T.; Xie, Y. Assessment of outdoor thermal comfort in Hong Kong based on the individual desirability and acceptability of sun and wind conditions. *Build. Environ.* **2018**, *145*, 50–61. [CrossRef]
2. Ng, E. Policies and technical guidelines for urban planning of high-density cities—Air ventilation assessment (AVA) of Hong Kong. *Build. Environ.* **2009**, *44*, 1478–1488. [CrossRef]
3. Hang, J.; Li, Y.; Buccolieri, R.; Sandberg, M.; DI Sabatino, S. On the contribution of mean flow and turbulence to city breathability: The case of long streets with tall buildings. *Sci. Total Environ.* **2012**, *416*, 362–373. [CrossRef] [PubMed]
4. Ng, E.; Cheng, V. Urban human thermal comfort in hot and humid Hong Kong. *Energy Build.* **2012**, *55*, 51–65. [CrossRef]
5. Hang, J.; Luo, Z.; Wang, X.; He, L.; Wang, B.; Zhu, W. The influence of street layouts and viaduct settings on daily carbon monoxide exposure and intake fraction in idealized urban canyons. *Environ. Pollut.* **2017**, *220*, 72–86. [CrossRef]
6. Du, Y.; Mak, C.M.; Liu, J.; Xia, Q.; Niu, J.; Kwok, K. Effects of lift-up design on pedestrian level wind comfort in different building configurations under three wind directions. *Build. Environ.* **2017**, *117*, 84–99. [CrossRef]
7. Tse, K.; Zhang, X.; Weerasuriya, A.; Li, S.; Kwok, K.; Mak, C.M.; Niu, J. Adopting 'lift-up' building design to improve the surrounding pedestrian-level wind environment. *Build. Environ.* **2017**, *117*, 154–165. [CrossRef]
8. Xia, Q.; Liu, X.; Niu, J.; Kwok, K.C.S. Effects of building lift-up design on the wind environment for pedestrians. *Indoor Built Environ.* **2017**, *26*, 1214–1231. [CrossRef]
9. Chew, L.W.; Norford, L.K. Pedestrian-level wind speed enhancement with void decks in three-dimensional urban street canyons. *Build. Environ.* **2019**, *155*, 399–407. [CrossRef]
10. Liu, J.; Zhang, X.; Niu, J.; Tse, K.T. Pedestrian-level wind and gust around buildings with a 'lift-up' design: Assessment of influence from surrounding buildings by adopting LES. *Build. Simul.* **2019**, *12*, 1107–1118. [CrossRef]
11. Fan, M.; Chau, C.K.; Chan, E.H.W.; Jia, J. A decision support tool for evaluating the air quality and wind comfort induced by different opening configurations for buildings in canyons. *Sci. Total Environ.* **2017**, *574*, 569–582. [CrossRef] [PubMed]
12. Du, Y.; Mak, C.M.; Tang, B.-S. Effects of building height and porosity on pedestrian level wind comfort in a high-density urban built environment. *Build. Simul.* **2018**, *11*, 1215–1228. [CrossRef]
13. Du, Y.; Mak, C.M. Improving pedestrian level low wind velocity environment in high-density cities: A general framework and case study. *Sustain. Cities Soc.* **2018**, *42*, 314–324. [CrossRef] [PubMed]
14. Muhsin, F.; Yusoff, W.F.M.; Mohamed, M.F.; Sapian, A.R. CFD modeling of natural ventilation in a void connected to the living units of multi-storey housing for thermal comfort. *Energy Build.* **2017**, *144*, 1–16. [CrossRef]
15. Du, Y.; Mak, C.M.; Huang, T.; Niu, J. Towards an integrated method to assess effects of lift-up design on outdoor thermal comfort in Hong Kong. *Build. Environ.* **2017**, *125*, 261–272. [CrossRef]
16. Sha, C.; Wang, X.; Lin, Y.; Fan, Y.; Chen, X.; Hang, J. The impact of urban open space and 'lift-up' building design on building intake fraction and daily pollutant exposure in idealized urban models. *Sci. Total Environ.* **2018**, *633*, 1314–1328. [CrossRef] [PubMed]
17. Zhang, X.; Tse, K.T.; Weerasuriya, A.U.; Li, S.W.; Kwok, K.C.S.; Mak, C.M.; Niu, J.; Lin, Z. Evaluation of pedestrian wind comfort near 'lift-up' buildings with different aspect ratios and central core modifications. *Build. Environ.* **2017**, *124*, 245–257. [CrossRef] [PubMed]

18. Du, Y.; Mak, C.M.; Li, Y. A multi-stage optimization of pedestrian level wind environment and thermal comfort with lift-up design in ideal urban canyons. *Sustain. Cities Soc.* **2019**, *46*, 101424. [CrossRef]
19. Zhang, X.; Tse, K.T.; Weerasuriya, A.U.; Kwok, K.C.S.; Niu, J.; Lin, Z.; Mak, C.M. Pedestrian-level wind conditions in the space underneath lift-up buildings. *J. Wind Eng. Ind. Aerodyn.* **2018**, *179*, 58–69. [CrossRef]
20. Chen, L.; Mak, C.M. Numerical evaluation of pedestrian-level wind comfort around "lift-up" buildings with various unconventional configurations. *Build. Environ.* **2021**, *188*, 107429. [CrossRef]
21. Gao, H.; Liu, J.; Lin, P.; Li, C.; Xiao, Y.; Hu, G. Pedestrian level wind flow field of elevated tall buildings with dense tandem arrangement. *Build. Environ.* **2022**, *226*, 109745. [CrossRef]
22. Chen, L.; Mak, C.M. Integrated impacts of building height and upstream building on pedestrian comfort around ideal lift-up buildings in a weak wind environment. *Build. Environ.* **2021**, *200*, 107963. [CrossRef]
23. Huang, Y.-D.; Ren, S.-Q.; Xu, N.; Luo, Y.; Sin, C.H.; Cui, P.-Y. Impacts of specific street geometry on airflow and traffic pollutant dispersion inside a street canyon. *Air Qual. Atmos. Health* **2023**, *15*, 1133–1152. [CrossRef]
24. Sin, C.H.; Luo, Y.; Jon, K.S.; Cui, P.-Y.; Huang, Y.-D. Effects of void deck on the airflow and pollutant dispersion in 3D street canyons. *Environ. Sci. Pollut. Res.* **2022**, *29*, 89358–89386. [CrossRef]
25. Chew, L.W.; Norford, L.K. Pedestrian-level wind speed enhancement in urban street canyons with void decks. *Build. Environ.* **2018**, *146*, 64–76. [CrossRef]
26. Sin, C.H.; Cui, P.-Y.; Jon, K.S.; Luo, Y.; Shen, J.-W.; Huang, Y.-D. Evaluation on ventilation and traffic pollutant dispersion in asymmetric street canyons with void decks. *Air Qual. Atmos. Health* **2023**, *16*, 817–839. [CrossRef]
27. Jiang, Z.; Gao, W. Impact of Enclosure Boundary Patterns and Lift-Up Design on Optimization of Summer Pedestrian Wind Environment in High-Density Residential Districts. *Energies* **2021**, *14*, 3199. [CrossRef]
28. Weng, J.; Luo, B.; Xiang, H.; Gao, B. Effects of Bottom-Overhead Design Variables on Pedestrian-Level Thermal Comfort during Summertime in Different High-Rise Residential Buildings: A Case Study in Chongqing, China. *Buildings* **2022**, *12*, 265. [CrossRef]
29. Zhang, X.; Gao, Y.; Tao, Q.; Min, Y.; Fan, J. Improving the pedestrian-level wind comfort by lift-up factors of panel residence complex: Field-measurement and CFD simulation. *Build. Environ.* **2023**, *229*, 109947. [CrossRef]
30. Aldawoud, A. Thermal performance of courtyard buildings. *Energy Build.* **2008**, *40*, 906–910. [CrossRef]
31. Gao, Y.; Yao, R.; Li, B.; Turkbeyler, E.; Luo, Q.; Short, A. Field studies on the effect of built forms on urban wind environments. *Renew. Energy* **2012**, *46*, 148–154. [CrossRef]
32. Moonen, P.; Dorer, V.; Carmeliet, J. Evaluation of the ventilation potential of courtyards and urban street canyons using RANS and LES. *J. Wind Eng. Ind. Aerodyn.* **2011**, *99*, 414–423. [CrossRef]
33. Yang, L.; Liu, X.; Qian, F.; Niu, S. Research on the wind environment and air quality of parallel courtyards in a university campus. *Sustain. Cities Soc.* **2020**, *56*, 102019. [CrossRef]
34. Al-Hemiddi, N.A.; Megren Al-Saud, K.A. The effect of a ventilated interior courtyard on the thermal performance of a house in a hot–arid region. *Renew. Energy* **2001**, *24*, 581–595. [CrossRef]
35. Rojas, J.M.; Galán-Marín, C.; Fernández-Nieto, E.D. Parametric Study of Thermodynamics in the Mediterranean Courtyard as a Tool for the Design of Eco-Efficient Buildings. *Energies* **2012**, *5*, 2381–2403. [CrossRef]
36. Micallef, D.; Buhagiar, V.; Borg, S.P. Cross-ventilation of a room in a courtyard building. *Energy Build.* **2016**, *133*, 658–669. [CrossRef]
37. Wen, Q.; Liu, H.; Chen, J.; Ye, H.; Pan, Z. Evaluation of Satisfaction with the Built Environment of University Buildings under the Epidemic and Its Impact on Student Anxiety. *Int. J. Environ. Res. Public Health* **2023**, *20*, 4183. [CrossRef] [PubMed]
38. Etheridge, D. A perspective on fifty years of natural ventilation research. *Build. Environ.* **2015**, *91*, 51–60. [CrossRef]
39. Buccolieri, R.; Sandberg, M.; Di Sabatino, S. City breathability and its link to pollutant concentration distribution within urban-like geometries. *Atmos. Environ.* **2010**, *44*, 1894–1903. [CrossRef]
40. Buccolieri, R.; Salizzoni, P.; Soulhac, L.; Garbero, V.; DI Sabatino, S. The breathability of compact cities. *Urban Clim.* **2015**, *13*, 73–93. [CrossRef]
41. Hang, J.; Wang, Q.; Chen, X.; Sandberg, M.; Zhu, W.; Buccolieri, R.; Di Sabatino, S. City breathability in medium density urban-like geometries evaluated through the pollutant transport rate and the net escape velocity. *Build. Environ.* **2015**, *94*, 166–182. [CrossRef]
42. Blocken, B.; Stathopoulos, T.; van Beeck, J. Pedestrian-level wind conditions around buildings: Review of wind-tunnel and CFD techniques and their accuracy for wind comfort assessment. *Build. Environ.* **2016**, *100*, 50–81. [CrossRef]
43. Zheng, X.; Montazeri, H.; Blocken, B. CFD simulations of wind flow and mean surface pressure for buildings with balconies: Comparison of RANS and LES. *Build. Environ.* **2020**, *173*, 106747. [CrossRef]
44. Lateb, M.; Masson, C.; Stathopoulos, T.; Bédard, C. Comparison of various types of k–ε models for pollutant emissions around a two-building configuration. *J. Wind Eng. Ind. Aerodyn.* **2013**, *115*, 9–21. [CrossRef]
45. Ai, Z.; Mak, C. Determination of single-sided ventilation rates in multistory buildings: Evaluation of methods. *Energy Build.* **2014**, *69*, 292–300. [CrossRef]
46. Tominaga, Y.; Mochida, A.; Yoshie, R.; Kataoka, H.; Nozu, T.; Yoshikawa, M.; Shirasawa, T. AIJ guidelines for practical applications of CFD to pedestrian wind environment around buildings. *J. Wind Eng. Ind. Aerodyn.* **2008**, *96*, 1749–1761. [CrossRef]
47. *GB 50178-93*; Standard of Climatic Regionalization for Architecture. China Academy of Building Research. China Planning Press: Beijing, China, 1994.
48. *GB50009-2012*; Load Code for the Design of Building Structures. China Construction Industry Press: Beijing, China, 2012.

49. Vervoort, R.; Blocken, B.; van Hooff, T. Reduction of particulate matter concentrations by local removal in a building courtyard: Case study for the Delhi American Embassy School. *Sci. Total Environ.* **2019**, *686*, 657–680. [CrossRef] [PubMed]
50. Qin, H.; Lin, P.; Lau, S.S.Y.; Song, D. Influence of site and tower types on urban natural ventilation performance in high-rise high-density urban environment. *Build. Environ.* **2020**, *179*, 106960. [CrossRef]
51. Niu, J.; Liu, J.; Lee, T.-C.; Lin, Z.; Mak, C.; Tse, K.-T.; Tang, B.-S.; Kwok, K.C. A new method to assess spatial variations of outdoor thermal comfort: Onsite monitoring results and implications for precinct planning. *Build. Environ.* **2015**, *91*, 263–270. [CrossRef]
52. Padilla-Marcos, M.; Meiss, A.; Feijó-Muñoz, J. Proposal for a Simplified CFD Procedure for Obtaining Patterns of the Age of Air in Outdoor Spaces for the Natural Ventilation of Buildings. *Energies* **2017**, *10*, 1252. [CrossRef]
53. Da Silva, F.T.; Reis, N.C.; Santos, J.M.; Goulart, E.V.; de Alvarez, C.E. The impact of urban block typology on pollutant dispersion. *J. Wind Eng. Ind. Aerodyn.* **2021**, *210*, 104524. [CrossRef]